CZECH UNIVERSITY OF LIFE SCIENCES PRAGUE

Faculty of Tropical AgriSciences

Department of Sustainable Technologies

Macroscopic analysis of biomass briquettes

Diploma thesis

Prague 2015

Supervisor:

Ing. Tatiana Ivanova, Ph.D.

Author:

Veronika Chaloupková

Declaration

I hereby confirm on my honour that the presented master thesis entitled "Macroscopic analysis of biomass briquettes" I have elaborated completely by myself and independently, solely with the expert and academic guidance of my thesis supervisor Ing. Tatiana Ivanova, Ph.D. I also declare that all sources of information and data that have been used are properly listed in the references at the end of the thesis or they are outcomes of my own laboratory research.

Prague, 24 April 2015

....

Veronika Chaloupková

Acknowledgement

Abstrakt

Biomasa z rostlin, zvláště zbytky ze zemědělské či lesnické výroby a energetické plodiny slouží jako slibný alternativní, obnovitelný a ekologicky šetrný zdroj pro výrobu energetických paliv. Densifikace, ve formě briketování, zvyšuje objemovou hmotnost rostlinného materiálu a produkuje pevná bio-paliva uniformní ve velikosti a tvaru, která mohou být snadněji a efektivněji manipulována, přepravována a skladována. V současné době je výroba vysoce kvalitních briket s dobrými mechanickými, chemickými a energetickými vlastnostmi silně žádoucí. Jedna z metod hodnocení kvality zrnitého/částicového materiálu je počítačové vidění a doprovodná analýza obrazu. Cílem předkládané práce je prostřednictvím obrazově založené makroskopické analýzy zanalyzovat a zhodnotit strukturu povrchu briket za účelem zjistit velikost částic a jejich rozložení a tak lépe pochopit vzorec chování vstupního materiálu při aglomeraci v lisovací komoře briketovacího stroje a identifikovat potenciální zásady a pravidla chování a interakce mezi částicemi v různých místech, jak na povrchu, tak i uvnitř briket vyrobených z různých rostlinných materiálů. Před briketováním, důležité vstupní parametry testovaných materiálů mající vliv na proces densifikace, tj. obsah vlhkosti a rozdělení velikosti částic, byly stanoveny na základě příslušných norem. Brikety vyrobené ze tří různých materiálů biomasy byly použity v rámci výzkumu; a to miscanthus (*Miscanthus* × *giganteus* L.), technické konopí (*Cannabis sativa* L.) a borovicové piliny (*Pinus* L.). Celkem 135 snímků bylo nasnímáno a kvalitativně i kvantitativně zanalyzováno. Pomocí Nis-Elements, softwaru pro analýzu obrazu, 900 délek a 900 ploch částic bylo změřeno. Získaná data byla statisticky zpracována a testována pomocí Kruskal-Wallisova testu (na hladině významnosti 0,05). Výsledky celkově ukázaly, že větší částice se vyskytují na přední straně briket, naopak menší částice ce koncentrují na zadní straně briket. Zároveň největší částice se nacházejí ve středu průřezů briket, zatímco nejmenší částice jsou umístěny ve spodní části briket.

Klíčová slova: strojové vidění, počítačové vidění, obrazová analýza, shlukování, struktura, lisování, velikost částic

Abstract

Biomass from plants, specifically agricultural or forestry waste and energy crops serve as promising alternative, renewable and environmentally friendly source for energy fuel production. Densification in terms of briquetting increases the bulk density of biomass material and produce uniform solid fuels in size and shape that can be more easily and efficiently handled, transported and stored. Nowadays the production of high-quality briquettes with good mechanical, chemical and energy properties is strongly desired. One of the methods for evaluating a quality of various granular/particulate materials is computer vision and accompanying image analysis. The aim of the presented work is via image-based macroscopic analysis to analyse and assess the briquette surface structure in order to determine particle size and its distribution, and thus better understand the behavioural pattern of input material during agglomeration process in the pressing chamber of briquette machine and to identify potential principles and rules in behaviour and interaction between particles at different locations on the surface as well as inside of the briquettes made of different sources of biomass material. Before briquetting important input parameters of tested feedstock materials affecting densification process, i.e. the moisture content and particles' size distribution, were determined according to the standards. The briquettes made of three different biomass materials were used within the research; namely miscanthus (*Miscanthus × giganteus* L.), industrial hemp (*Cannabis sativa* L.) and pine sawdust (*Pinus* L.). In total, 135 images were scanned and qualitatively as well as quantitatively analysed. Using Nis-Elements, software for image analysis, 900 lengths and 900 areas of particles were measured. Obtained data were statistically processed and tested by Kruskal-Wallis test (with significance level 0.05). The results showed that larger particles are generally on the front side of briquettes and *vice versa* smaller are on the rear side as well as larger particles are centred in the briquette cross-sections and smaller particles are located on the briquette bottom.

Key words: machine vision, computer vision, image analysis, agglomeration, structure, compaction, particle size

Table of contents

List of tables

List of figures

List of abbreviations

BEC	Biomass Energy Centre
CCD	Charge-coupled device
CEN	European Committee for Standardization
CULS	Czech University of Life Sciences Prague
CV	Computer vision
FE	Faculty of Engineering
FTA	Faculty of Tropical AgriSciences
ICT	Institute of Chemical Technology Prague
MC	Moisture content
MV	Machine vision
PC	Personal computer
PSD	Particle size distribution
RGB	Colour model (red, green, blue)
RIAE	Research Institute of Agricultural Engineering
SEM	Scanning electron microscopy
2D	Two-dimensional space (image)
3D	Three-dimensional space (image)

List of symbols

°C	Degree Celsius
$f(x, y)$	Image function, x and y represents pixel coordinates
g	Gram (unit of weight)
k	Bit depth
$kg.m^{-3}$	Kilogram per cubic metre
kW	Kilowatt
m_w	Total mass of wet material
m_d	Dry matter mass of the dried material
mm	Millimetre
mm/"g"	Sieve shaker intensity (vibration height in mm or acceleration of the sieve in "g" – acceleration due to gravity $9.81 m.s^{-2}$)
MPa	Megapascal
$m.s^{-1}$	Meter per square second (acceleration)
$(M \times N)$	Image resolution (width $\times$ height of the image matrix)
nm	Nanometre
px	Pixel
R^2	Coefficient of determination (R-squared)
$t.ha^{-1}$	Ton per hectare
μm	Micrometre
$μm.px^{-1}$	Micrometre per pixel
w.b.	Wet basis moisture content
α	Significance level
ρ	Density
ε	Porosity
$(1 - ε)$	Solids content

1 Introduction

Improving a quality of life, economic and industrial expansion as well as population growth bring with it serious problems related to energy sector (Hiloidhari *et al.*, 2014). As a result, the increasing demand for energy, and, along with the limited supplies of conventional fuels (especially fossil fuels) and their negative environmental impact lead the population to search for renewable and sustainable energy sources (Shaw, 2008; Carels, 2011; Kreuger *et al.*, 2011; Karunanithy *et al.*, 2012).

Due to these reasons there is increasing interest both in developed and developing countries in biofuels made of different types of biomass including agricultural wastes and energy crops as a perspective, sustainable and primarily renewable alternative energy source to conventional fossil fuels (Shaw, 2008; Tumuluru *et al.*, 2010; Alaru *et al.*, 2011; Carels, 2011; Vaezi *et al.*, 2013; Zhang and Guo, 2014). Densification of biomass into durable solid compacts is an effective solution to meet the need of law bulk density of raw materials for biofuels production (Kaliyan, 2008; Shaw, 2008; Kaliyan and More, 2009; Tumuluru *et al.*., 2010; Tabil *et al.*, 2011; Karunanithy *et al.*, 2012). Briquetting, the pressing and compacting under the high pressure, is one of the fundamental and promising methods of the processing of waste and purposely grown biomass and production of solid biofuels for combustion purposes (Tumuluru *et al.*, 2010). Currently, the production of high-quality briquettes as well as other bio-fuels which abounding with good mechanical, chemical and energy properties is strongly desired (Shaw, 2008).

One of the method by which quality of solid biofuels can be nowadays observed is computer/machine vision and image analysis. It is a highly useful and effective technique with versatile range of application in various areas of industry and science (Brosnan and Sun, 2002; Korbářová, 2009). It can be utilized in fields such as medical diagnostic and biotechnology (Tonar *et al.*, 2003), nanotechnology, automatic manufacturing and surveillance, remote sensing, technical diagnostics, safety technologies, autonomous vehicle and robot guidance (Brosnan and Sun, 2002; Korbářová, 2009). Above all, machine vision is used to increase efficiency and quality of controlled products and thus is characterized by a focus on typical image analysis tasks associated with managing the production process, including mainly visual inspection of prescribed visible parameters, identification of size, shape, colour, structure and texture, object counting, finding defects,

and, reading and verification of texts and codes (Chen *et al.*, 2002; Korbářová, 2009). Applications of this artificial vision based technique have expanded also to research of biomass materials for energy fuel production, where it is highly useful and effective tool for e.g. observation of surface and/or interior structures of briquettes as well as other heterogeneous materials. It represents another approach to analyse quantitatively particle size and its distribution as well as surface area of particulate material (Wang, 2006; Igathinathane *et al.*, 2009a; Igathinathane *et al.*, 2009b; Souza and Menegalli, 2011; Kumara *et al.*, 2012; Gil *et al.*, 2014; Pothule *et al.*, 2014; Pons and Dodds, 2015).

The aim of the thesis is to analyse a macrostructure of briquettes made from different sources of biomass materials, namely miscanthus, industrial hemp and pine sawdust through microscope technologies equipped with special software for the image processing and data measurement. This image-based macroscopic analysis which is focused on analysis and assessment of the briquette surface structure so as to determine particle size and its distribution and better understand the behavioural pattern of input material in the pressing chamber of briquetting machine and to observe if there are any principles and rules in behaviour and interaction between particles at different locations on the briquette surface within different sources of biomass material.

Knowledge of agglomeration process of raw input material during the pressing process is critical in the understanding the briquetting process as well as controlling the manufacturing operation. It can help to improve modes, parameters and technological conditions of equipment for briquette production and, above all, may ensure required high quality biofuels with appropriate technological properties according to the given standards.

2   Literature review

The theoretical part of this work is a fundamental insight into the whole issue – "Macroscopic analysis of biomass briquettes" and is divided into two main parts. First one is focused on objects studied in the thesis research – biomass briquettes. Firstly, plant biomass and its composition are generally described. Further chapter is focus on plant biomass in relation to energy production, with special regard to agricultural and forestry wastes and energy crops. The main attention is directed to densification process and especially to its products – briquettes, and their particles' agglomeration process and binding mechanisms during briquetting, as well as their structure and particle features.

The second part of the literature review is focused on a main method used in research to examine the studied objects – image analysis. Firstly, human vision and its principles are briefly mentioned, further special attention is paid to an artificial vision. Both computer vision and machine vision are presented, their principles and use, with special regard to utilization in studying of biomass material for energy purposes.

Part I.

2.1   Plant biomass – what is it?

Generally, the term biomass means "*biological material derived from living, or recently living organisms, both animal and vegetable*" (Tumuluru *et al.*, 2011a; BEC, not dated). In the context of biomass intended for energy production purposes the term usually refers just to plant based material, such as wood and herbaceous material (BEC, not dated). In this way the term biomass is understood within presented work and thus plant based material is hereafter referred to only as biomass. Biomass, the term used for all organic material originated from plants, including trees, crops and algae (McKendry, 2002), is a material that stems from the reaction among carbon dioxide in the air, water and energy of the sunlight, through photosynthesis process, to produce carbohydrates which form the structural framework of the biomass (McKendry, 2002). Thus, plant cell walls are the output of catching and transforming solar energy into chemical energy of rich polymers – carbohydrates through carbon fixation in the course of photosynthesis process (Faik, 2013).

2.2   Biomass composition

Biomass is a highly porous cellular material, of which the plant cells inside are comprised primarily of a large vacuole filled with water, or air in case of dried material (Stelte *et al.*, 2011). The plant cell wall is a composed of lignin, hemicellulose and cellulose and minor amounts of extraneous substances (McKendry, 2002; Pérez *et al.*, 2002; Wiemann, 2010; Faik, 2013). The content of these components in the plant depends on plant species (Jeffries, 1994) and furthermore the composition of plant cell wall (roots, stems, leaves) varies within the same plant according to age, stage of growth and other factors which affect the plant's life cycle (Jeffries, 1994; Sarkar *et al.*, 2009). Variances in plant cell wall composition have been ascertained in organs, cell types inside one tissue and moreover inside one particular cell (Knox, 2008; Frei, 2013).

However in general, dry biomass contains 40–50% cellulose, 20–25% lignin, 15–25% hemicellulose and 5–10% other components (McKendry, 2002; Faik, 2013). The relative proportions of these major components represent important determinative factors in identifying the suitability of plant species for subsequent converting to energy source (McKendry, 2002). Many authors have researched the biomass composition, e.g. Jeffries (1994), Pérez *et al.* (2002), Knox (2008), Sarkar *et al.* (2009), and Frei (2013). Veveris and co-authors (2004) studied lignin and cellulose content of various highly productive, non-wood plants and agricultural residues, including miscanthus, giant reed or switchgrass.

Cellulose

Cellulose is the main component of the biomass and thus the most abundant natural polymer in the world (Fengel and Wegner, 1983; Shaw, 2008; Stelte *et al.*, 2011). It is a structural component of plant cell walls of all plants from highly developed trees to primitive organisms like algae (Fengel and Wegner, 1983). Its amount in plant varies from species to species (Fengel and Wegner, 1983). High content of cellulose occurs in natural fibres – cotton, kapok, jute, flax, hemp etc. On the other hand, low content can be found in mosses or barks (Fengel and Wegner, 1983). Wood contains 40–50% of cellulose (Fengel and Wegner, 1983; Fujita and Harada, 2000; Pérez *et al.*, 2002). Ververis *et al.* (2004) examined the content of cellulose as well as lignin and ash in several types of high-productive and non-wood plants and agricultural residues.

From chemical point of view, cellulose is unbranched polymer with the molecular formula $(C_6H_{10}O_5)_n$ consisting of many chains of β-1,4 linked glucose units (Fengel and Wegner, 1983; Pérez *et al.*, 2002; Pietsch, 2002; Shaw, 2008; Kumar and Turner, 2014). These chains, linked together by hydrogen bonds and van der Waals forces (Pézer *et al.*, 2002), are arranged into ordered strands of high crystallites generally called as microfibrils (Suchy, 2011). In association with the other elements, the microfibrils are arranged into fibers which are the main structural components of the plant cell wall (Stelte *et al.*, 2011). Cellulose occurs in the primary and secondary cell wall, proportionally more represented is in the secondary cell wall (Pérez *et al.*, 2002).

Hemicellulose

Another component of plant cell wall, which is closely associated to cellulose, is hemicellulose (Pérez *et al.*, 2002; Stelte *et al.*, 2011). It is highly branched polysaccharide of β-1,4 (and occasionally β-1,3) linked glucose units (Scheller and Ulvskov, 2010; Stelte *et al.*, 2011) with lower molecular weight than cellulose (Pérez *et al.*, 2002). The main components of hemicellulose are D-xylose, D-mannose, D-galactose, D-glucose, L-arabinose, 4-O-methyl-glucuronic, D-galacturonic and D-glucuronic acids (Pérez *et al.*, 2002; Scheller and Ulvskov, 2010). Hemicelluloses are linked by hydrogen bonds to the surface of cellulose microfibrils. It differs from cellulose in having branches with short lateral chains comprising of different carbohydrates (Pérez *et al.*, 2002).

Structure and abundance of hemicellulose differ according to species and cell types. Hemicellulose contributes to strengthening the cell wall by interaction with cellulose, and in some cases, with lignin. Hemicellulose occurs in the primary and secondary cell wall, however proportionally is more represented in the primary cell wall (Scheller and Ulvskov, 2010).

Lignin

Another important component of the plant cell walls is lignin (McKendry, 2002; Pérez *et al.*, 2002; Wiemann, 2010). It is highly complex amorphous polymer containing phenylpropane units (Pérez *et al.*, 2002; Rowell *et al.*, 2012), namely mainly guaiacyl, sinapyl and p-hydroxyphenyl, that are linked by aryl ether or C-C bonds (Zeng *et al.*, 2014). The content of lignin in plant cell wall depends on many factors, as is mentioned above. The content of this polymer in one specific plant can differ (Jeffries, 1994; Sarkar *et*

al., 2009) according to stage of growth, genotype, kind of organ and environmental conditions (Knox, 2008; Frei, 2013). Customarily, lignin detection can be done by histochemical staining, Raman microscopy or using ultraviolet light to generate blue fluorescence (Kaliyan and Morey, 2010; Zeng *et al.*, 2014).

From physical point of view, lignin helps to increase strength of the cell wall (Fujita and Harada, 2000; Stelte *et al.*, 2011). Therefore, it is found in plant cell walls, where it has supporting and mechanical functions and also serves as resistant against microbial attack and oxidative stresses (Pérez *et al.*, 2002). However, the role of lignin in terms of energy production can be called as ambiguous (Frei, 2013). On the one hand, thermally softened lignin acts as binding agent in conversion of biomass to solid bio-fuel (briquettes, pellets) which joints particles together and thus contributes considerably to the strength characteristics and causes the finished product more durable (Granada, 2002; Kaliyan and Morey, 2009; Chou *et al.*, 2009; Kaliyan and Morey, 2010). Biomass with a higher content of lignin, protein or starch is characterized by better compaction than those with higher cellulosic content (Tumuluru *et al.*, 2011b). On the other hand Zeng *et al.* (2014) reviewed negative roles of lignin in the biomass conversion processes, including chemical pre-treatment, microbial fermentation, and enzyme hydrolysis.

Extraneous components

Besides these major components, biomass contains also extraneous components (McKendry, 2002; Wiemann, 2010). They represent a wide range of chemical compounds, which generally comprise only a small part of plant material (Fengel and Wegner, 1983). Some plant species, e.g. grasses, contain high amounts of these components, like waxes, that are of hydrophobic nature and situated in the plant's cuticula, where they have a role of protection, or spruce possesses tall lipid containing many hydrocarbon derivates (Stelte *et al.*, 2011).

2.3   *Biomass as a source of energy*

Nowadays, there is worldwide increasing interest in the use of biomass as a perspective, sustainable and especially renewable source of energy (Li and Liu, 2000; Shaw, 2008; Tumuluru *et al.*, 2010; Alaru et al, 2011; Carels, 2011; Pothula *et al.*, 2014). It is especially important in order to reduce the production of greenhouse gases, biological waste and also to meet still increasing energy demand to avoid dependence on gradually

exhausting fossil fuels (Li and Liu, 2000; McKendry, 2002; Kaliyan and More, 2009; Tumuluru *et al.*, 2010; Karunanithy *et al.*, 2012; Zhang and Guo, 2014). Attractiveness of biomass (if properly managed) resides in its renewability and sustainability, abundance and local availability, and positive environmental effect due to carbon-neutrality and very low sulphur content (Tumuluru *et al.*, 2010; Carels, 2011; Karunanithy *et al.*, 2012; Pothula *et al.*, 2014).

2.3.1 *Types of plant biomass for energy purposes*

As was mentioned before, due to the increased demand for energy as well as limited supplies of fossil fuels there is increasing interest in biofuels made of different types of biomass as a perspective, sustainable and primarily renewable alternative energy source to conventional fuels (Shaw, 2008; Tumuluru *et al.*, 2010; Alaru *et al.*, 2011; Carels, 2011). Biomass sources for energy production include a wide range of materials which can be classified according to many criteria such as source of biomass or type of conversion process (Tumuluru *et al.*, 2011a). However, in this work we will focus mainly on biomass material suitable for production of solid biofuels.

Least expensive biomass sources are the waste products from wood as well as agriculture harvesting and processing operations (Tumuluru *et al.*, 2010; Tumuluru *et al.*, 2011a; Alaru *et al.*, 2011; Carels, 2011). It includes wood – material from wood processing or from forestry activities such as sawdust, wood shavings, barks, as well as agricultural biomass wastes – residues from agriculture harvesting or processing like husks and straw from cereals (e.g. rice, maize or wheat), sunflower husks, coffee husks, cotton stalks, coir pith, sugar beet leaves, waste flows from bulb sector (Grover and Mishra, 1996). However, the supplies of these waste resources are limited. To overcome these obstacles, the energy crops – high yielding crops grown mainly for energy purposes are more and more cultivated and used for energy production to utilize the biomass material more efficiently. The energy crops are comprise of dry lignocellulosic woody crops such as poplar, willow or eucalyptus; dry lignocellulosic herbaceous crops like miscanthus, hemp, common reed, giant reed, switccgrass, cynara cardu, aanary grass or indian shrub (Tumuluru *et al.*, 2011a).

Woody and herbaceous energy biomass sources, namely miscanthus, industrial hemp and pine sawdust, are the types of biomass examined in this study; we can call them

as lignocellulosics. It can be defined as "*plant cell wall biomass composed primarily of cellulose, hemicelluloses and lignin*" (BS EN ISO 16559, 2014). Lignocellulosic biomass has become more and more important as a source of energy, which is not competitive to food production (Somerville *et al.*, 2010). Pérez *et al.* (2002) reviewed new advances in the various biological treatments which can convert these three the most abundant biopolymers on the Earth into alternative fuels.

2.4 The need for densification

Biomass, in its original form, is characterized by high moisture content, which ranges from 10 up to 70%, irregular shape and sizes, and low bulk density[1] of 30 kg.m^{-3} (Mani *et al.*, 2006a). Thus, due to these factors, large biomass quantities are difficult and inefficient to handle, store, transport and utilize in its original form without some kind of pre-processing (Kaliyan, 2008; Shaw, 2008; Kaliyan and More, 2009; Tumuluru *et al.*, 2010; Stelte *et al.*, 2011; Karunanithy *et al.*, 2012). To make the raw biomass accessible and suitable for a diverse uses, the challenges with the use of these raw materials must be resolved (Kaliyan and More, 2009). Based on the biomass material, there are many processes available for conversion of raw biomass into a more convenient form and into what is called as a "biomass fuel" or "bio-fuel" (Tumuluru *et al.*, 2011a; BEC, not dated).

One of the method which offers promising solution to overcome the mentioned obstacles and limitations of raw input materials is mechanical densification of biomass into pellets, briquettes or cubes (Grover and Mishra, 1996; Kaliyan, 2008; Shaw, 2008; Kaliyan and More, 2009; Tumuluru *et al.*, 2010; Igathinathane *et al.*, 2010; Tabil *et al.*, 2011; Karunanithy *et al.*, 2012). Densification of biomass is achieved by forcing the loose particles together into a larger, more compact form, by application of mechanical force to cause particle-to-particle bonding (Wamukonya and Jenkins, 1995; Tabil, 1996; Pietsch, 2002; Shaw, 2008; Kaliyan and More, 2010). According to the standards (BS EN ISO 16559, 2014) densified biofuel can be defined as "*solid biofuel made by mechanically compressing biomass or thermally treated biomass to mould the solid biofuel into a specific size and shape such as cubes, pressed logs, biofuel pellets or biofuel briquettes*". In this thesis attention is mainly paid to biofuel briquettes.

---

[1] Bulk density is defined as "*the weight the unit volume of a particulate mass under non-specific condition, e.g. in storage or in a shipping container*" (Pietsch, 2002) or as "*ratio of the mass and the volume of a sample including pore volume*" (Rabier *et al.*, 2006).

[2] True density means "*the mass of the unit volume of a solid material that is free of pores*" (Pietsch, 2002).

Densification increases the bulk density of biomass material up to 600–800 kg.m^{-3} (Kaliyan and More, 2009) and produce uniform products in size and shape that can be more easily and efficiently handled, transported and stored and thus it reduces the costs associated with these operations (Grover and Mishra, 1996; Kaliyan, 2008; Kaliyan and More, 2009; Kaliyan and More, 2010; Karunanithy *et al.*, 2012). Moreover owing to unitary and regular shape and size, with densified products can be without problems manipulated using the standard handling and storage equipment and also they can be with ease used in direct combustion, pyrolysis, gasification, as well as in other biomass-based conversion processes (Kaliyan and More, 2009). Besides these benefits, densified products have higher energy density, they are dry and can be stored without degrading and thus they have higher sales value (Kaliyan, 2008).

Before the densification process, reduction of particles' size is essential to enlarge the total surface area, size of material porosity and increase the quantity of contact points for inter-bonding among particles (Drzymala, 1993; Shaw, 2008) and thus increase mechanical strength of the compacts (Zhang and Guo, 2014). Such feedstock material ground to a required particle size can be then underwent to other pre-treatment processes like mixing with additives and fats, or exposed to steam conditioning and expansion for the purpose of increasing the temperature and moisture content of the feed material (Thomas and van der Poel, 1996). Characteristics of the feedstock material like mentioned particle size, moisture content and usage of binders as well as characteristics associated with densification equipment which include pressure, speed of compression, die temperature, die shape and size affect densification process of biomass materials (Kaliyan, 2008; Tumuluru *et al.*, 2010).

A lot of researchers have studied densification of herbaceous and woody biomass using piston or screw presses (Tumuluru *et al.*, 2010). Chou and co-workers (2009) analysed the optimum conditions for preparing the solid fuel briquettes from the rice straw by a piston-mold process. Granada *et al.* (2002) studied the biomass densification mechanism and developed new die for a hydraulic press for briquetting. Li and Liu (2000) in their study performed high-pressure piston-and-mold compaction process to densify the wood processing residues and other biomass waste materials.

Several national standards characterize particle density of pressed products (briquettes/pellets) as an indicator of its quality. Many authors including Chin and Siddiqui

(2000), Rabier *et al.* (2006), Kaliyan and More (2009), Ivanova (2012), Zhang and Guo (2014) researched the quality of the densified products in terms of briquette/pellet strength, stability and durability. Efficiency of a densification process to generate strong and durable bonding between particles within densified products can be appointed by testing the strength (i.e. water resistance, compressive resistance, and impact resistance), and durability (that is abrasion resistance) of the compacted products (Kaliyan and More, 2009). Highly durable and stable densified products are less susceptible to damage during handling, transportation and storage operations (Mani *et al.*, 2006b).

2.5 *Briquetting – process of compaction*

Briquetting, process of forming briquettes, is the most known and widely spread technology of materials compaction (Kers *et al.*, 2010). Densification of loose biomass waste or purposely cultivated plants using briquetting press is feasible and appealing solution to employ biomass for energy fuel production (Tumuluru *et al.*, 2010). Briquetting is one of the applications of pressure agglomeration methods during which the biomass is compressed under high pressure and temperature which arise from the high friction between the biomass and the press channel walls (Tabil, 1996; Pietsch, 2002; Shaw, 2008; Tumuluru *et al.*, 2010; Kers *et al.*, 2010).

In the compaction process – briquetting, three following phases of deformation takes place: structural, elastic and plastic (Tabil, 1996; Pietsch, 2002; Shaw, 2008; Muntean *et al.*, 2013). (I.) Initially particle rearrangement occurs at low pressures to break down the unstable packing arrangement of discrete particles and result to a denser balanced formation. The physical properties of the particles are kept. (II.) Elastic and plastic deformation, which occurs during application of higher pressures, leads to particle flow into empty spaces, elimination of the air and increase contact among particles. In this stage, the sizes and shapes of the raw material particles are not modified or just to a limited extent (III.) Particle fracture and rearrangement lead to mechanical interlocking for brittle materials. Both phases (II.) and (III.) continue till the true density[2] is acquired. Local melting arises if the temperature exceeds the particular melting points. In the case of biomass and biological materials, pressure acts at the same time on the tissue's morphology, cell organelles, membranes, and at the molecular level (Shaw, 2008).

---

[2] True density means "*the mass of the unit volume of a solid material that is free of pores*" (Pietsch, 2002).

Final product of briquetting, briquette, is defined as "*densified biofuel made with or without additives in the form of cubiform, polyhedral, polyhydric or cylindrical units with a diameter of more than 25 mm, produced by compressing biomass*" (BS EN ISO 16559, 2014). Pietsch (2002) determinates briquettes as "*agglomerates produced and shaped by high-pressure agglomeration process*". The biomass briquettes are clean and green biofuels which can be combusted in furnaces, boilers or in open fire (Tumuluru *et al.*, 2010). Briquettes have a specified shape according to the applied compaction method/process and the shape of stamping die (Pietsch, 2002; Ivanova, 2012). They can have shape of cylinders, prisms or hexahedrons with diameter 40–100 mm and length up to 300 mm independently on the material (Stupavský and Holý, 2010).

Many studies have been conducted to prepare the biomass briquettes from agricultural and forest residues (Chou *et al.*, 2009). For example, Chin and Siddiqui (2000) densified biomass material, including sawdust, rice husks, peanut shells, coconut fibres and palm fruit fibres, into briquettes using a piston and die type presses. Coates (2000) in his study use cotton plant residues to produce briquettes. Yaman *et al.*, 2000 investigated production of the briquettes using olive refuse. Or Husain and co-workers (2002) in their study briquetted palm fibre and shell residues from the processing of palm nuts to palm oil. Stolarski *et al.* (2013) evaluated the possibility of producing briquettes from agricultural and forest biomass as well as determined their quality and the production costs. Srivastava *et al.* (2014) investigated the energy use of briquettes from vegetable market waste. As well as other authors studied potential of various types of grown biomass for briquette production, e.g. perennial grasses, such as *Caragana korshinskii* Kom (Zhang and Guo (2014), miscanthus (Ivanova, 2012), giant knotweed, switchgrass (Kaliyan and Morey, 2010) and giant reed (Ivanova, 2012); annul plants – hemp fibre (Alaru *et al.*, 2011; Ivanova, 2012), sunflower (Alaru *et al.*, 2011) or corn stover (Kaliyan and Morey, 2010).

Major factors determining the properties of briquettes, as well as other agglomerates, are already mentioned: particle size and distribution, shape, surface area, size and shape of briquette, true and bulk density, porosity, size of pores and their distribution in the densified product, moisture content, and last but not least strength (Pietsch, 2002; Kaliyan, 2008; Tumuluru *et al.*, 2010). Moisture content of feedstock material as well as particle size are fundamental input parameters for compaction (pressing) process and they have considerable influence on briquettes quality (Grover and

Mishra, 1996; Zhang and Guo, 2014). Zhang and Guo (2014) in their study investigated influence of input parameter such as pressure, temperature, moisture content and size of particles on the physical properties, i.e. durability, density, compressive strength and impact resistance, of briquettes made of *Caragana korshinskii* Kom. Karunanithy *et al.* (2012) studied physiochemical characterization of briquettes made of different feedstocks. Demirbas *et al.* (2004) in his study investigated properties of briquetting including moisture content, shatter index, water resistance, compressive strength, heating value, and combustion of briquettes made of spruce wood sawdust and pulping reject.

2.6   *Process of agglomeration*

Generally, agglomeration is a natural process of the pasting loose solid particles together, which is associated with application of short-range physical or chemical forces among the particles themselves, by physical or chemical modifications of the solids that are set off by certain process conditions, or by binding agents, substances which adhere chemically or physically to the solid surfaces and develop a material bridge between the particles (Pietsch, 2003). The principal import of agglomeration process resides in improving of specific physical characteristics of solid materials, including bulk density, dispersibility, and stability (Pietsch, 2002; Pietsch, 2003). Agglomeration can be done by pressure, tumble/growth and/or heat/sintering technology (Pietsch, 2002). Further attention of this thesis is focused just on pressure agglomeration technology.

2.6.1 *Binding mechanisms between particles*

Generally, the binding mechanisms (i.e. physical and chemical effects causing adhesion and bonding between solid surfaces) of agglomeration which work between the constituent particles in products during densification can be divided according to classical theory into five main categories: (i.) solid bridges, (ii.) adhesion and cohesion forces, (iii.) surface tension and capillary pressure, (iv.) attraction forces between solids, and, (v.) mechanical interlocking bonds (Rumpf, 1962; Pietsch, 2002).

If the high pressures and temperatures are applied, the solid bridges can be formed by diffusion of atoms or molecules from one particle to another at the points of contact. Solid bridges between particles can be developed owing to chemical reaction, hardening of bonding agents, crystallization of dissolved materials, and solidification of melted substances as well; see Figure 1 (Rumpf, 1962; Pietsch, 2002). Solid bridges are primarily

developed after drying or cooling of products which went through the process of densification (Kaliyan and Morey, 2009). Most finely divided particles of solids attracting with ease free atoms or molecules comprise fine adsorption layers which are not mobile and which may develop strong bonds between contiguous particles. This is done by both smoothing out surface roughness and raising the contact area between particles or by diminishing the inter-particle distance and enabling to the intermolecular attractive forces to partake in the bonding mechanism (Ghebre-Sellassie, 1989). Strongly adhesive binding agents, such as molasses and bitumen, adhere to the surfaces of solid particles to create strong bonds which are greatly resemble to those of solid bridges. A lot of viscous binding agents harden after cooling and develop the solid bridges (Pietsch, 2002). Occurrence of liquids like free moisture among particles, particularly in a wet agglomeration process[3], brings about cohesive forces between particles (Grover and Mishra, 1996). Solid particles may attract one another through short-range forces, such as molecular (valance and van der Waals'), magnetic, or electrostatic forces, which may give rise adhesion of solid particles to each other if the particles are got close enough together. Throughout the compression process, fibres, flat or irregularly shaped as well as bulky particles may weave, twist, and bend about each other leading to mechanical interlocking bonds (Pietsch, 2002; Kaliyan and Morey, 2009).
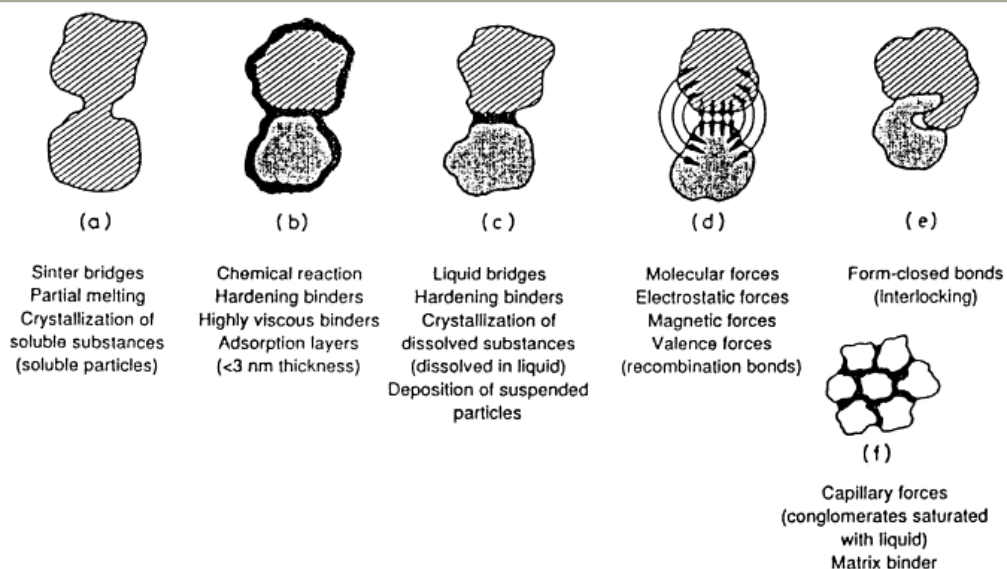
Figure 1: The binding mechanisms of agglomeration process
Source: Pietsch, 2003

---

[3] Wet agglomeration poses tumble and growth agglomeration process in which the main binding agent is a liquid (Pietsch, 2002).

These binding forces have been detected and posited e.g. during the densification of pharmaceutical powder materials (Ghebre-Sellassie, 1989), animal feeds (Tabil, 1996), and biomass materials as well (Lindley and Vossoughi, 1989; Kaliyan and Morey, 2009). Binding mechanisms in wood and wood products summarized Back (1987). According to his study, hydrogen bonding at lignin and cellulose surface areas is accountable for the major kind of bonding mechanism in the press-drying process of wood processing.

2.6.2 Binding agents

The biomass materials contain various amounts of natural binders (binding agents) in it, such as water soluble carbohydrates, lignin, protein, starch and fats, (Kaliyan, 2008; Chou *et al*., 2009; Kaliyan and Morey, 2010). These natural binders are activated at high pressures and temperatures during densification to act as local binders of particles. After densification process, when pressure and temperature are ceased, the natural binders harden or "set up" forming bridges or bonds between particles, which results in binding them together and thus causes the finished biofuel more durable (Kaliyan and Morey, 2010). It overcomes already mentioned limitations caused by the need to obtain sufficient strength for transport, handling, packaging, and storage operations of densified products (Pietsch, 2002; Shaw, 2008). As was stated above, water also acts as a film type binder during the densification process by strengthening the bonding in briquettes. Water supports development of bonding by van der Waals' forces by increasing the inter-particle contact area (Grover and Mishra, 1996; Pietsch, 2002). Sundry studies showed that strength and durability of the densified products increased with increasing moisture content till an optimum value is achieved (Kaliyan and Morey, 2009).

Many studies have presented that different biomass feedstock have good binding properties without using additives (Shaw and Tabil, 2007); such biomass grinds have own natural binding agents which allow them to manifest preferred assets after densification process (Shaw, 2008). Wamukonya and Jenkins (1995) studied the possibility of producing durable binderless briquettes from wheat straw and sawdust. Li and Liou (2000) investigated high-pressure compaction of wood processing residues as well as other biomass waste materials, such as hardwood, softwood, and bark in the forms of sawdust, mulches, and chips without adding binding agents. Kaliyan and Morey (2010) in their research studied the role of natural binders in switch grass and corn stover to make durable particles' bonding mechanisms in briquettes and pellets.

2.7   *Briquette structure*

A structure of briquettes is of high importance for all briquettes' properties. Structure of final product is highly influenced by applied process – tumble/growth agglomeration, pressure agglomeration and heat/sintering agglomeration; it differs according to mechanisms predominating in these processes (Pietsch, 2002). In case of pressure agglomeration, the structure is influenced by mentioned phases of deformation and primarily depends on level of densification (Pietsch, 2002). In pressure agglomeration process, externally rendered forces act on loose material in pressing chamber and die defines the shape of a final briquette (Tumuluru *et al.*, 2010).

The structure of briquettes also rests on many different parameters that are associated to the particles building and all the processes engaged in formation the raw material and output agglomerate. Especially during high-pressure agglomeration process and diverse post-treatment operations parameters associated with the raw input particles may transform (Pietsch, 2002). Composition of input feedstock has one of the largest impacts on the final briquette structure. The most important particle-related factors influencing briquette structure are: particle size and its distribution, macroscopic as well as microscopic shape of particle – e.g. roughness (Pietsch, 2002; Muntean *et al.*, 2013).

Briquette structure can be observed by scanning the image of the cross-section which may provide information and knowledge on particle size and its distribution, porosity (ε), content of solids ($1 - \varepsilon$), and, with the use of suitable software, a shape factor and the particles' specific surface area (Pietsch, 2002). Accurate range can be extended by studying multiple cuts through the same product and ascertaining the statistical means for all of them (Pietsch, 2002). Scanning electron microscopy (SEM) is highly useful and effective tool for the observation of surface and/or interior structures of briquettes as well as other solid materials (Pietsch, 2002). Zhang and Guo (2014) using SEM studied structure of briquettes made from perennial grass *Caragana korshinskii* Kom in terms of porosity. Kaliyan and Morey (2010) used SEM and light microscopy to analyse micro-structural bonding mechanisms in briquettes and pellets made from corn stover and switchgrass. Stelte *et al.* (2011) examined fracture surfaces of beech pellets using also SEM to obtain deeper knowledge about bonding mechanism between particles. Computer vision and associated image analysis is another approach for observation and quality assessment (Korbářová, 2009).

2.7.1 Particle size and shape

Owing to the high share of cellulose, hemicellulose and lignin in the biomass content, the shape of particles is significantly irregular (Guo *et al.*, 2012). Information and understanding of particle morphology are important in the areas related to particle handling, transport, mixing, fluidization or combustion (Gil *et al*., 2014). Muazu and Stegemann (2015) using SEM studied morphology of rice husks and corn cobs particles intended for briquette production. Guo *et al.* (2012) studied the particle shape of four kinds of biomass materials quantitatively by images analysis, and researched the particle size distributions using sieving method.

Size of particles significantly affects the physical properties of briquettes (Zhang and Guo, 2014). Investigations of Lu *et al.* (2010) indicate that particle shape and size influence biomass particle dynamics, including drying, heating rate, and reaction rate. Particle size and particle size distribution (PSD) also play important roles in flow ability, bulk density, compressibility of bulk solid material, and durability of densified products (Grover and Mishra, 1996; Ganesan *et al.*, 2008; Kaliyan and Morey, 2009). Reducing particle size leads to increasing density, durability, impact resistance and decreasing compressive strength (Zhang and Guo, 2014). In general, the finer grind, the higher durability, albeit small-sized particles create more durable briquettes, fine grinding is undesirable due to increased cost of production (Kaliyan and Morey, 2009).

PSD analysis is considered as a standard method to assess the dimensional characteristics and morphological features of particulate materials (Igathinathane *et al.*, 2009a; ČSN EN 15149-1, 2011; Vaezi *et al.*, 2013). Generally, outputs from PSD analysis comprise percentage of particles captured on sieves with diverse opening sizes, cumulative undersize distribution, geometric and arithmetic mean value and related standard deviation, as well as many other parameters which in unique way characterize the distribution of particles (Igathinathane *et al.*, 2009a). PSD of biomass can be determined by various procedures, including traditional mechanical screening (sieve analysis) as well as newly used image analysis method (Igathinathane *et al.*, 2009b; Gil *et al.*, 2014). More information about this method, which could be considered as an alternative or even a replacement for traditional sieve analysis approach (Igathinathane *et al.*, 2009b), are presented in the second part of the thesis.

Part II.

In the foregoing part of the literature review object of our interest – biomass briquettes has been described. The briefer second part of the review is focused on a main method used to examine the briquettes within the research – artificial vision-based image analysis. Firstly, human vision and its principles are briefly mentioned, however main attention is paid to an artificial vision. The core of artificial vision, digital image is also touched on. Above all, computer vision/machine vision is presented, its principles and use, with special regards to biomass material for energy purposes.

3.1 Vision – the challenge

Before inquiring directly into to the issues of artificial vision and specifically image analysis we have to gain very brief insight into the base itself – natural vision, the incomparable model and inspiration for artificial vision systems. Vision, one of the five human senses, is the dominant sense by which human-being receives most of data from surrounding environment (Davies, 2005; Russ, 2006; Erichsen and Woodhouse, 2012; Sonka *et al.*, 2014). Every person who is able to perceive the world visually performs almost in every moment of his life (except maybe sleep) image analysis of the world around him (Korbářová, 2009). Information from visual perception is our most natural and inherent source of information and communication (Gevers *et al.*, 2012).

Vision starts with the organ which is sensitive to light – eye (Korbářová, 2009; Erichsen and Woodhouse, 2012). Man obtain visual features of the image such as colour, orientation, and luminance from light which reaches the eye by photoreceptor and ganglion cells in the retina (Korbářová, 2009; Mohr *et al.*, 2014). Due to the existence of three types of cones in the retina, that are sensitive to different areas of the visible spectrum, is in principle human vision tricolour. Each colour perceived by eye can be expressed as a mixture of three independent primary colours. This property of human vision is imitated by colour models that are used in display devices for expressing various colours of the spectrum (Korbářová, 2009). As we can see from Figure 2, visible light is only a narrow section of the whole electromagnetic radiation spectrum (Russ, 2006; Erichsen and Woodhouse, 2012; Sonka *et al.*, 2014).
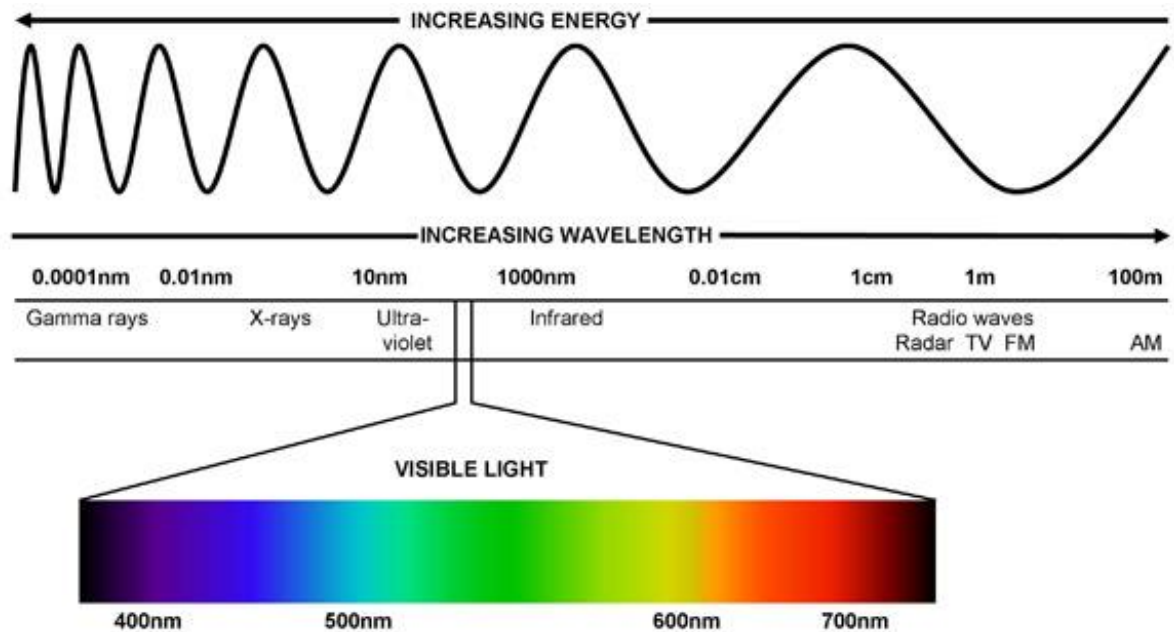
Figure 2: The spectrum of light wavelengths which are visible to humans

Source: Harrington, 2010

3.2   *Digital image – object of analysis*

Images are at the core of vision, both natural and artificial (Davies, 2005). Even before we focus on the main part of this thesis part, which is machine vision and image analysis, is necessary to mention the cornerstone of the whole issue – the digital image. In order to analyse and evaluate the digital image, it is necessary to know its properties, ways of expression and the possibility of transformation (Korbářová, 2009). The most complicated image is colour one, which is also the most frequently starting element of the analysis (Korbářová, 2009), so our attention is mostly paid on it. Colour of the digital image can be described through several models describing the entire colour spectrum, which can be imagined as three-dimensional (3D) coordinate systems, where each colour is represented by a precisely defined point (Fiřt and Holota, 2002). The most commonly used colour model is a system called RGB, according to the initial letters of the English names of the three primary colours (Red, Green, Blue), whose combination is used to describe all colours of the spectrum. This model can be presented as a cube placed at the beginning of the 3D coordinate system (Fiřt and Holota, 2002; Korbářová, 2009).

In the field of image analysis instead of the term digital image is often used only short term – image (Korbářová, 2009), and so it will be understood throughout this thesis. Digital image in this work is construed as a two-dimensional (2D) array of pixels (px/picture elements), i.e. values representing the light intensity of each point (Fisher *et al.*, 2014). Mathematically, an image can be described as a two-variable function $f(x, y)$, where x and y are spatial coordinates of particular pixel (Fiřt and Holota, 2002; Korbářová, 2009).

Digital image can be described by three basic characteristics: resolution, bit depth and number of colour levels (Korbářová, 2009). Image resolution, unit of the digital image, means "*the number of pixels per unit area*" (Fiřt and Holota, 2002; Fisher *et al.*, 2014). The size (quality) of an image is given by the width M (number of columns) and the height N (number of rows) of the image matrix (Fiřt and Holota, 2002; Burger and Burge, 2009). In other words, image size is determined by the total number of pixels (M × N) which forms an image (Korbářová, 2009). Image resolution is considered as the ability of digital image to duplicate fine details which have occurred in the original scene. Bit depth is a number of bits used for decoding the pixel value. If the bit depth is k, then one pixel can take 2^k different values. In professional applications is mostly used colour depth of 8 bits for monochrome images (256 shades of gray) and 24 bits for colour ones, that corresponds to what is seen in the real scene (Fiřt and Holota, 2002). Number of colour levels in an image describes how many pixels networks together form a complete picture (Korbářová, 2009). A greyscale or monochrome images are created only by one colour level, while the full-colour images (true-colour) are composed of three layers corresponding to the three primary colours: red, green and blue (Korbářová, 2009, Fiřt and Holota, 2002).

3.3 Artificial vision

As mentioned before, vision enables men to perceive and understand the world around them (Davies, 2005; Russ, 2006; Erichsen and Woodhouse, 2012; Sonka *et al.*, 2014). However, human vision, sophisticated though it is, has some limitations (Batchelor and Bruce, 2012). Apart from human vision, there is artificial vision, which also deals with the understanding of visual information (Gevers *et al.*, 2012). This visual information plays an essential and vital role in today's society and is the core of present communication frameworks (Korbářová, 2009; Gevers *et al.*, 2012). Artificial vision, such as computer vision and/or machine vision, endeavours to copy the effect of human vision by electronic perceiving and understanding an image (Sonka *et al.*, 2014; Zhang and Li, 2014).

According to Batchelor and Bruce (2012) "*Artificial Vision is concerned with the analysis and design of opto-mechanical-electronic systems that can sense their environment by detecting spatio-temporal patterns of electro-magnetic radiation and then process that data, in order to perform useful practical functions*". In other words, artificial vision deals with the processing and analysis of images using electronic equipment.

Mentioned above, there are two terms associated with artificial vision – computer vision (CV) and machine vision (MV). Many authors of technical literature use those terms synonymously, the CV is often used to denote MV, and *vice versa* (Snyder and Qi, 2004; Batchelor and Bruce, 2012; Zhang and Li, 2014). On the contrary, other authors consider these terms as representatives of distinct fields. Batchelor and Bruce (2012) assert that the MV is related to, however distinct from CV; notwithstanding, there is common terminology, concepts and algorithmic techniques for MV and CV.

3.3.1 Computer & machine vision – areas of utilization

Computer vision is a relatively new discipline. Explosion of interest and concentrated works in the field appeared at the end of the 1970s, when the computer technology allowed to process large amounts of data, which carry image information (Brosnan and Sun, 2002; Davies, 2005; Szeliski, 2011; Zhang and Li, 2014). Generally, this term currently refers to systems that operate automatically on the basis of information obtained from image analysis and processing, which is created through the sensing element in the camera or other optical device (Davies, 2005; Korbářová, 2009). CV encompasses a wide area of topics that often intersect with other disciplines, thus there is no general formulation "tasks of CV". The object of CV can be basically anything, e.g. transport situation, the human face/body and human activities, but primarily it is evaluation and control of a production processes (Korbářová, 2009).

Currently, for CV used in industrial production is usually chosen the term MV. In the past few decades, MV has made enormous progresses (Shen *et al.*, 2012). According to Batchelor and Bruce (2012) MV "*is concerned with the engineering of integrated mechanical-optical-electronic software systems for examining natural objects and materials, human artifacts and manufacturing processes, in order to detect defects and improve quality, operating efficiency and the safety of both products and processes. It is also used to control machines used in manufacturing*". It is characterized by a focus on

typical image analysis tasks associated with managing the production process. These tasks include mainly visual inspection of prescribed visible parameters, identification of size, shape, colour, structure and texture, object counting, finding defects, and, reading and verification of texts and codes (Chen *et al.*, 2002; Korbářová, 2009). Applications of these artificial vision based techniques have expanded to various fields such as medical diagnostic and biotechnology (Tonar *et al.*, 2003), nanotechnology, automatic manufacturing and surveillance, remote sensing, technical diagnostics, safety technologies, autonomous vehicle and robot guidance (Brosnan and Sun, 2002; Korbářová, 2009). However, MV is primarily used to increase efficiency and quality of controlled of products (Korbářová, 2009). In varying degrees, it is used in diverse industries (Brosnan and Sun, 2002), including automobile, food and agricultural, textile, and, pharmacy industry.

Determination of quality of materials/products is important to secure good and satisfactory utilization of resources from economic and environmental point of views (Kumara *et al.*, 2012). Digital image processing and analysis have also been utilized to investigate various properties of engineering materials, including metal, plastics, glass, wood, ceramics, rubber, and concrete (Batchelor and Bruce, 2012; Kumara *et al.*, 2012). In case of concrete, micro-structural analysis, crack length and fracture characteristics (Shah and Kishen, 2011), strain and displacement distributions (Kutay *et al.,* 2006), particle flow and pore size distribution (Yang *et al.*, 2009) can be investigated by artificial vision. Ozen and Guler (2014) also used image analysis for determination of micro-structural properties, aggregate size and shape characteristics, air voids distribution, and the PSD of concrete.

PSD analysis using image-based analysis is one of the used procedures for quality evaluation of various granular/particulate materials (Igathinathane *et al.*, 2009b; Kumara *et al.*, 2012; Vaezi *et al.*, 2013). This CV based method can be considered as an alternative or even a replacement for traditional screening method (Igathinathane *et al.*, 2009b). Image analysis is the technique that is sensitive to the geometrical shape for determining a more precise measure of size together with shape (Fernlund, 1998). As mentioned, Ozen and Guler (2014) determined the PSD of aggregates from 2D cross-sectional images of concrete samples. Mora *et al*. (1998) analysed PSD of coarse aggregates using image processing. Or Kumara *et al.* (2012) evaluated PSD of gravel by image analysis technique.

It can be also used for studying of sedimentary rocks – identification and quantification of minerals, pores and textures. For example, Berrezueta *et al.* (2015)

identified morphological parameters of pores and grain spaces of sandstones. Karakuş *et al.* (2010) analysed size and shape of minerals using image processing.

The artificial vision based technique of quality inspection has also found applications in the agricultural and food industry (Brosnan and Sun, 2002). The images of agricultural and food products, obtained using the image analysis techniques, can be quantitatively characterised by a set of features, such as size, shape, colour, and texture (Du and Sun, 2006). It includes the inspection and grading of fruit (Bato *et al.*, 2000; Xiao-bo *et al.*, 2010; Matiacevich *et al.*, 2011; Vanloot *et al.*, 2014) and vegetable (Wooten *et al.*, 2000). It has also been used successfully in the evaluation of foods such as meats (Lu *et al.*, 2000; Park and Chen, 2001; Trinderup *et al.*, 2015), aquatic products, including fish, shrimps and oysters (Dowlati *et al.*, 2012; Hong *et al.*, 2014), cheese (Wang and Sun, 2001), bakery products (Abdullah, 2000; Farrera-Rebollp *et al.*, 2011) and pizza (Sun, 2000). MV has been applied also within grain classification and quality evaluation of cereals (Brosnan and Sun, 2002). E.g. Lloyd *et al.* (2000) evaluated both milled rice from a laboratory mill and a commercial-scale mill for head rice yield and percentage whole kernels, with use of a shaker table and a MV system. Walker and Panozzo (2012) developed digital imaging method to determine the size, weight, volume and density of individual barley grains. Colour and size uniformity are important grading and evaluating factors for many food products. Shahin *et al.* (2006) determined size uniformity of soya bean seeds via image processing. Du and Su (2006) reviewed promise techniques for food and agricultural products quality assessment using artificial vision. Further, Sarrafzadeh *et al.* (2015) evaluated biomass concentration of three types of microalgae. Zhang and Li (2014) reviewed basic concepts, components, and image acquisition modes of CV techniques in case on inspection of cotton. Besides inspection, grading and evaluation of the products, MV technology can be used also for land-based and aerial-based remote sensing for natural resources evaluation, precision agriculture, detection of product safety, classification and sorting, and process automation (Chen *et al.*, 2002).

As we see from the versatility of this technique in various fields of industry and science, its development is still on the rise. It is still possible to find ways of improvement both in the development of the basic elements of the system (sensing elements, illuminators, software) and solving of the specific image analysis tasks (Korbářová, 2009).

3.3.2 Image analysis in studies of biomass materials for energy purposes

In case of biomass materials for energy purposes, application of the artificial vision and image analysis is limited to a few areas, e.g. for analysis of particle size and shape (Wang, 2006; Pothule *et al.*, 2014; Pons and Dodds, 2015). Pons and Dodds (2015) described steps and examples of image analysis of particles, from image acquisition, processing, to measuring operations in binary image. As was mentioned, these techniques are characterized by high accuracy, non-invasiveness and no sample consumption, and can be used PSD analysis as alternative or even replacement of traditional screening method (Igathinathane *et al.*, 2009a; Igathinathane *et al.*, 2009b; Souza and Menegalli, 2011; Kumara *et al.*, 2012; Gil *et al.*, 2014). Vaezi and co-workers (2013) used image processing for PSD within the analysis of lignocellulosic biomass for pipeline hydro-transportation. Gil *et al.* (2014) applied CV and image analysis for to characterization of the standard sieving method in order to determine which particle dimension is being measured (in case of poplar and corn stover). Doehlert *et al.* (2004) compared and evaluated size uniformity of oat kernels by both digital image analysis and sequential sieving method. Womac *et al.* (2007) measured geometric mean dimensions of switchgrass by image analysis also compared with traditional sieve based approach. Febbi *et al.* (2015) determined poplar chip PSD and particles dimension based on combined image and multivariate analyses.

Besides PSD analysis, image-based technique can be applied to quantification of particle shape (Pons and Dodds, 2015). Guo and co-workers (2012), who used image analysis for studying the particle shape of four kinds of biomass materials. Iganthinathane *et al.* (2010) measured volume, surface area and density of cotton gin trash briquettes, switchgrass pellets, switchgrass cubes, hardwood pellets, and softwood chips using 3D laser scanner. Wooten and co-workers (2011) discriminated bark from wood chips through texture analysis by image processing. Pan and Kudo (2011) determined the distribution shapes of pores and information on the positions and sizes of pores of wood by image analysis. Pothula *et al.* (2014) identified nodes and internodes of chopped biomass stems of corn stover, switchgrass and big bluestem biomass stems, by digital image processing. Or Carlsson and co-workers (2013) submitted two types of lignocellulosic biomass particles, European spruce and American hardwood to very high heating rates and simultaneously used a high-speed camera to capture the behaviour of the biomass particle during the heating process.

3.4   *Process of machine vision*

MV solves the analytical tasks almost analogously as a human (Korbářová, 2009; Zhang and Li, 2014). The sensing element (e.g. camera) captures, like the human eye, the image of the object or scene, the system evaluates it according to the specified algorithm and performs the action specified by measurement results. Generally, principle of MV can be described as a feedback system in which the sensor is composed of a camera and the resulting image evaluation, management and control of the reporting process provides mostly computer and the accompanying equipment (Korbářová, 2009). Schematic diagram of the MV process chain is shown in Figure 3. Generally, the image analysis technique includes an analysis, by means of a computer, illumination system, scanning device, and obtained two-dimensional images. Parameters defined by computer software are measured quickly and precisely. The obtained outputs can be subsequently listed in a table or plotted in graphic form (Fernlund, 1998; Zhang and Li, 2014).

| Real object | ▸ | Image acquisition | ▸ | Image record | ▸ | Image processing | ▸ | Image analysis | ▸ | Presentation of results |

Figure 3: Scheme of machine vision

Source: Korbářová, 2009

Object of the vision

The object, which is analysed using MV, can be both real object (a specific product) and process that needs to be monitored or controlled (Korbářová, 2009). In this work entry element will be the real object (briquette) as mentioned, however analysis of manufacturing processes is nearly analogous. In general, an object has to be optically distinguishable. This means that the object must be able to reflect the falling radiation, to sufficient record of required information on obtained 2D image (Korbářová, 2009).

Image acquisition

The first essential step and cornerstone of the image analysis is image acquisition/capture of the real world, its conversion into digital form suitable for storage and further processing in a computer or other system (Fiřt and Holota, 2002; Davies, 2005; Ozen and Guler, 2014; Fisher et al, 2014). Before image acquisition itself, it is necessary to

select the optimal combination of these parameters affecting the brightness, contrast, or even colour of the image. They are: the type of lighting (its intensity, colour, shape of the light beam, the dynamic behaviour of light, etc.), then the lens aperture sensing element and the exposure time (Korbářová, 2009). Lighting of monitored object plays a key role in obtaining quality images (Korbářová, 2009; Zhang and Li, 2014).

As was mentioned, image capture is acquisition of image scene by recording device, e.g. camera, and converted into a digitized form and send it to computer for recording (Fiřt and Holota, 2002; Davies, 2005; Ozen and Guler, 2014; Fisher *et al.*, 2014). It is the transfer of the optical variable into an electrical signal, which is continuous in both time and level (Fiřt and Holota, 2002). There are various imaging devices, e.g. plumbicons, vidicons, dissectors and CCDs (charge-coupled devices). Nowadays, the CCDs are the mostly used (Snyder and Qi, 2004). All these mentioned imaging devices convert the light energy to voltage in resembling ways (Snyder and Qi, 2004).

Image processing and analysis

The acquired and digitized image is subsequently processed with the special software (e.g. Nis-Elements, MATLAB) for the image analysis which contains library of functions allowing various ranges of image modifications and their evaluation (Korbářová, 2009). The aim of this phase is to adjust the image into a form suitable for the purpose of the analysis (Chen *et al.*, 2002). Generally, image processing can be used for two aims: improvement of visual appearance of images to human view, or preparation of images for feature measuring (Russ, 2006). For the correct carrying out of the MV, necessary software tools are as follows: image balance, image calibration, morphological changes of image, working with image colour, measurements and evaluation (Korbářová, 2009).

Function of image balance is to increase the quality of the final image with respect to highlight the details that are subjected to analysis and thus suppress undesirable effects. It can include: focus or blur the image, adjust the edges of objects or reduce image noise, change the brightness and enhance contrast of colours, or gamma correction (Korbářová, 2009; Zhang and Li, 2014). Image calibration is necessary for real measurements of objects in the image. It assigns real size to image information expressed in pixels. This is done mainly using a reference object which has a defined size and is taken under exactly the same conditions as the image (Korbářová, 2009; Fisher *et al.*, 2014). Colour image adjustment functions include locating and comparing colours, extraction of colours,

filtration and image thresholding. The last one, thesholding, is a function which converts the initial image to image binary. It is type of image, where pixels *"can be either an "on" or an "off" state, represented by integers 1 and 0 respectively"* (Fisher *et al.*, 2014), in other words it is an image whose pixels can have only two values, usually black and white colour, however it may be any two values of the entire colour spectrum. Morphological functions, such as filling apertures and/or particles removal, are tools for editing of object shape in an image. They usually work with a binary image where search areas with the same value of the pixel, adapt them according to preset algorithms and analyze them (Korbářová, 2009).

The last step of the whole procedure is measurement itself. It includes tools for making measurements in the image, which usually analyse geometric figures and that by seeking their edges and determining the distance. Most often lengths of studied objects are measured, less frequently areas. Software for image analysis is often able to measure the distances and angles between objects. It is necessary to reiterate that in order to determine the real length units, the image should be subjected to the above mentioned image calibration (Korbářová, 2009). A substantial part of the functions are also tools filtering objects with certain properties and setting their number. In this last stage of image analysis there are used features that are not able to work even with colour or grey scale images, so they have to be preceded by converting to binary image (Korbářová, 2009; Fisher *et al.*, 2014). Figure 4 shows the use of multiple features in the image which measures dimensions of a metal component within binary image in both the edge distance and the aperture diameters, and the angle of cut on the lower part of the product.

a)   b)
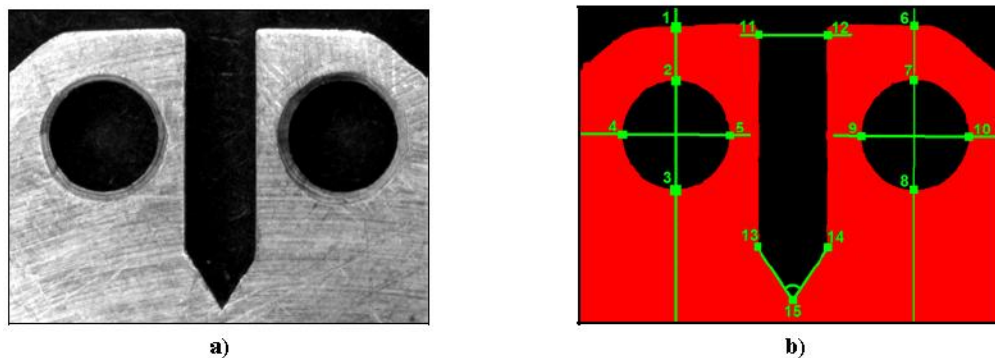
Figure 4: Measuring of dimensions via Nis-Elements software
Notice: a) initial image, b) binary image with measurements

Source: Korbářová, 2009

4 Hypothesis and objectives of the thesis

4.1   Hypothesis

The hypothesis for this thesis, formulated based on experience and observations gained throughout previous studies of solid biofuels and literature review elaboration, has run as follows:

(i.)   "*the smallest particles of the biomass material are found at the bottom of the briquettes while the largest particles are present on top of the briquettes*" (bottom and top of the briquettes is meant in relation to the passing of compacting material through die, i.e. bottom of briquette = bottom of die, and *vice versa,* top of the briquette = top of the die).

4.2   Overall objective

The main aim of the thesis have been to analyse a macrostructure of briquettes made from different kinds of biomass materials, namely industrial hemp, miscanthus and pine sawdust.

4.3   Specific objectives

The overall objective of the thesis is supported and supplemented by the specific objectives that are set so as to help to fulfil the main objective. The specific objectives of the thesis had been defined as follows:

(i.)   to determine input parameters, moisture content and particle size distribution, of selected biomass materials;

(ii.)   to produce briquettes made of these different sources of biomass;

(iii.)   to analyse briquettes' surface structure and identify principle of agglomeration during the pressing process of raw materials;

(iv.)   to determine particles' size and their distribution on the briquette surface under macroscopic conditions.

5 Methodology

5.1 *Methodology of literature review*

For elaboration of the literature review, theoretical part of the thesis, available sources and literature of both Czech and primarily foreign authors of scientific articles and books were used. The articles were obtained from scientific databases, mainly from Science Direct, Scopus and Web of Science and were searched based on combination of keywords: biomass, briquettes, image analysis, machine vision, computer vision, agglomeration, compaction, pressing process, structure and particle size. The used scientific articles were published in journals including mainly: Biomass and Bioenergy, Powder technology, Bioresource Technology and Computers and Electronics in Agriculture.

5.2 *Methodology of practical research*

Methodology of the practical research was based on quantitative as well as qualitative research methods and included these parts:

5.2.1 *Materials*

In this study, briquettes made of three following biomass materials were produced and used for research purposes: industrial hemp (*Cannabis sativa* L.), miscanthus (*Miscanthus × giganteus* L.) and pine sawdust (*Pinus* L.). Miscanthus was chosen because it has good potential as a biomass energy crop (Hodkinson and Renvoize, 2001; Hodkinson *et al.*, 2002), and nowadays is subjected to intense research and discussion. Industrial hemp is annual fibre plant which utilization for energy purposes is interesting alternative. And pine sawdust as wood material represents traditional feedstock for solid biofuels production (McKendry, 2002), thus also this material have been included to the study. The concise description of selected biomass materials is as follows:

Cannabis sativa **L.**

Industrial hemp (hereafter referred to as hemp) is annual herbaceous fibre crop from family *Cannabaceae* with C_3 photosynthesis originated from Western Asia and India which produces high above ground biomass yields (16–20 t.ha^{-1} of dry matter), and has low-intensive and high-adaptable cultivation (Kreuger *et al.*, 2011).

***Miscanthus* × *giganteus* L.**

Miscanthus is a genus of large perennial rhizomatous grasses of *Poaceae* family with C_4 photosynthesis, which origin is in the East Asia (McKendry, 2002; Clifton-Brown *et al.*, 2004; Dufossé *et al.*, 2014) and which is widely cultivated as a promising source of biomass for renewable energy production (Hodkinson and Renvoize, 2001; McKendry, 2002; Hodkinson *et al.*, 2002). *Miscanthus* × *giganteus* L. (hereafter referred to as miscanthus) can grow up to 3–4 meters and yield annually 20 to 50 t.ha^{-1} for early harvests and 10 to 30 t.ha^{-1} for late harvest of dry matter (Lewandowski *et al.*, 2000; Clifton-Brown *et al.*, 2000; Clifton-Brown *et al.*, 2004).

The above stated energy crops were cultivated in the experimental plots of CULS and harvested in the spring 2014. After harvesting, the biomass materials were naturally dried out to the moisture content suitable for storage.

Pine sawdust

The last studied biomass material for briquette production and subsequent macroscopic analysis was wood sawdust, especially mixture of pine (approximately 90%) and spruce (ca. 10%). In view of the fact that the share of pine (*Pinus* L.) is significantly predominant, the material is hereafter referred to as pine sawdust. The material was obtained as waste product from the CULS joinery and therefore nothing more about its origin is known.

5.2.2 Methods

5.2.2.1 Grinding – pre-treatment of the material for briquetting

During autumn 2014, at laboratory of Faculty of Engineering (FE) at Czech University of Life Sciences Prague (CULS), dry above-ground plant biomass of hemp and miscanthus was ground by hammer mill 9FQ-40C (manufactured by Pest Control Corporation company; input 5.5 kW). The materials were ground with one hammer mill screen size 12 mm. No other components were added to ground biomass. The pine sawdust was not ground, since it was the waste material and thus had already been disintegrated.

5.2.2.2 Determination of moisture content

The moisture contents (MC) of ground materials were measured according to the ČSN EN 14774-2 (2010) standards using the oven drying method at laboratory of the Faculty of Tropical AgriSciences (FTA) at CULS. For each biomass kind, a small amount

of material was finely grinded (by laboratory grinding machine), putted into two weighed Petri dishes and then together weighed again. All weightings were performed on the digital laboratory scale KERN (model EW 3000-2M) with readout 0.01 g. Then, the weighed samples were placed into the oven MEMMERT model 100-800 (Schwabach, Germany), see Figure 5, and dried out within 2.5 hours at 105 ℃. After drying process, the filled Petri dishes were removed from the oven, cooled in a desiccator about 15 minutes to room temperature and reweighed. The weights of Petri dishes were subtracted from the weight of cooled samples and moisture contents (in %) were then calculated using the following formula:

$$MC = \frac{(m_w - m_d)}{m_w} \times 100\%$$

where: MC   - moisture contents wet basis (%),

m_w - wet material mass (g),

m_d - dry matter mass of the dried material (g).

The final results were calculated as the arithmetic means of the two measurements for each material type.

Figure 5: Oven MEMMERT model 100-800 and digital laboratory scale KERN
Source: Author, 2014

5.2.2.3 *Particle size distribution measuring*

Prior to briquetting process, at laboratory of the FTA, a sieve analysis, according to the ČSN EN 15149-1 (2011) norms, was used to determine distribution of particles size. For this purpose horizontal sieve shaker Retsch AS 200 was used together with seven sieves and a bottom pan (< 0.63). The sieves have had following opening sizes/ apertures: 0.63, 1.5, 3.15, 4.5, 6.7, 8 and 10 mm, and were arranged from the largest (on the top) to the smallest opening sizes (on the bottom) on the shaker. Figure 6 shows mechanical shaker with the ordered sieves and bottom pan. On every biomass material, the two same tests (repetitions) were applied. Before testing, all sieves as well as bottom pan were weighted on the laboratory scale KERN (readout 0.01 g). For each test, representative weighed sample from each biomass material was poured into the top sieve with the largest screen opening size and 30-minute sieve shaking time and amplitude 30 mm/"g" was used for each test. After shaking process, each sieve with captured material was weighted and weight of sieves themselves was subtracted. The captured weight of the sample on the each sieve was calculated as an arithmetic mean of these two measurements (tests). This result from each sieve was then divided by the total weight (i.e. arithmetic mean of two input weights of material) to give a percentage of material retained on each sieve.

Figure 6: Horizontal sieve shaker Retsch AS 200 used for PSD analysis
Source: Author, 2015

5.2.2.4 Briquetting

During winter 2014/2015 the ground material was subsequently pressed to the form of fuel briquettes. Briquetting was carried out at the Research Institute of Agricultural Engineering (RIAE) Prague and the FE CULS[4]. At the RIAE ground material of hemp and miscanthus was pressed by hydraulic piston briquetting machine BrikStar CS 50 (shown in Figure 7), manufactured by Czech company Briklis, with diameter 65 mm of pressing cylinder, which corresponds approximately to the diameter of produced briquettes; length of produced briquettes ranged from 30 to 50 mm. The BrikStar briquetting press works under maximum compression pressure 18 MPa and maximum pressing temperature 60 ˚C (Briklis, not dated)[5]. At the FE the raw pine sawdust was briquetted using also hydraulic piston briquetting press BrikStar model CS 50.

Figure 7: Hydraulic piston briquetting press BrikStar CS 50 at RIAE
Source: Author, 2014

All briquettes were prepared without any additional binding agents at room temperature. During briquetting process 20 consecutive briquettes from each biomass material (in total 60) were selected and marked on the lateral top (for the easier identification of press-output position). The selection was carried out in the middle of briquetting process when stronger briquettes were produced. From these selected

---

[4] Due to technical obstacles (reconstruction of the FE premises) the briquetting had to be done at two places, however with the same type of briquetting press (i.e. with identical technical parameters).
[5] Other technical parameters and scheme of the briquetting press BrikStar are presented at the same source.

briquettes, five of them (non-consecutive)[6] were picked out for macroscopic analysis and numbered from 1 to 5. Their length and diameter were measured by electronic digital caliper; the diameter at the marked lateral top and opposite side of briquette (it corresponds to points A and C, expressed in later subchapter) and the length at the marked lateral top as well (Figure 8). After the image analysis, these five briquettes were cut transversally in the middle to produce two equally-sized cylinders for further image analysis of inner structure.
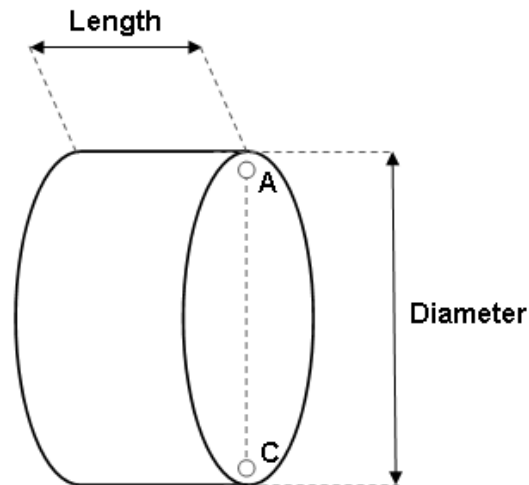
Figure 8: Measuring of length and diameter of examined briquettes

5.2.2.5 Image-based macroscopic analysis

The produced briquettes were subjected to image-based macroscopic analysis aimed to analyse and assess the briquette cross-sectional surface structure in order to determine particle size and its distribution and better understand the behavioural pattern of input material during agglomeration process in the pressing chamber of briquetting machine and to identify potential principles and rules in behaviour and interaction between particles at different locations on the surface as well as inside of the briquette within different sources of biomass material.

System setup

For purpose of this study, the laboratory of image analysis at the Department of Physics and Measurements of Institute of Chemical Technology Prague (ICT) was used for macroscopic analysis of biomass briquettes. Following hardware (Figure 9) and software equipment was employed to the research: stereomicroscope Zeiss Stemi 2000 equipped with illumination Schott VisiLED MC1500, Sony digital camera DFW-SX 910 with CCD

---

[6] The rest briquettes were used for initial trials.

detector of resolution 1392×1040 pixels, personal computer (PC), IC Capture 2.3 (software for image capturing), above all Nis-Elements Advanced Research 3.2, special software for the image processing and data measurement, further Microsoft Office Excel 2007, and statistical software Statistica 12.
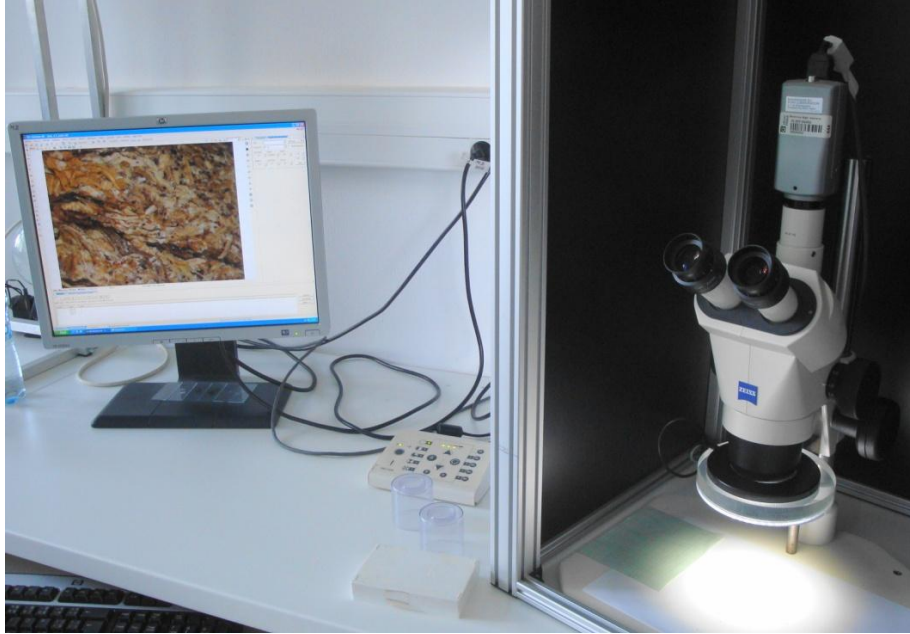
Figure 9: Equipment for macroscopic analysis (ICT Prague)
Source: Author, 2014

Process of image analysis

In the laboratory, the selected briquettes of each material's kind were observed via stereomicroscope and scanned by digital camera through IC Capture software. Firstly, the briquette was put under microscope objective and illuminated by white LEDs. Then the images of cross-sections (i.e. fractured surfaces) were taken, with 6.5 times magnification. From each briquette nine images were scanned, which means 45 images from every biomass source were obtained (five briquettes, nine measured points), and in total 135 colour 2D images, which were subsequently used for qualitative analysis and assessment of briquette structure, and thereafter for quantitative analysis using measurement tools.

Firstly, the briquettes were scanned on the surface at six specific points (A, B, C, D, E, F), which you can see on the scheme of Figure 10. The points A, B, C were placed on the front side (Figure 10a), which is breaking area of the briquettes outletting from briquette press (arrows indicate the direction and position of the briquettes leaving from

press die). Points D, E, F were located at the rear side (Figure 10b), where piston pressed during briquetting (compaction). Points A, C, D, and F were placed approximately five millimetres from the briquette edge (top and bottom), and points B and E in the middle of the circular cross-section. After scanning of these six surface points, to observe inside structure the briquettes were cut by electric band saw (brand Bomar) into two equal halves, thus two equal cylinders were created from each briquette. On the inner side of one half of the briquette three scanned points (G, H, I) were placed, as you can see in Figure 10c. The locations of these points were same as the previously scanned points, i.e. G and I five millimetres from the briquette edge (top and bottom), and points H in the middle of the circular cross-section.
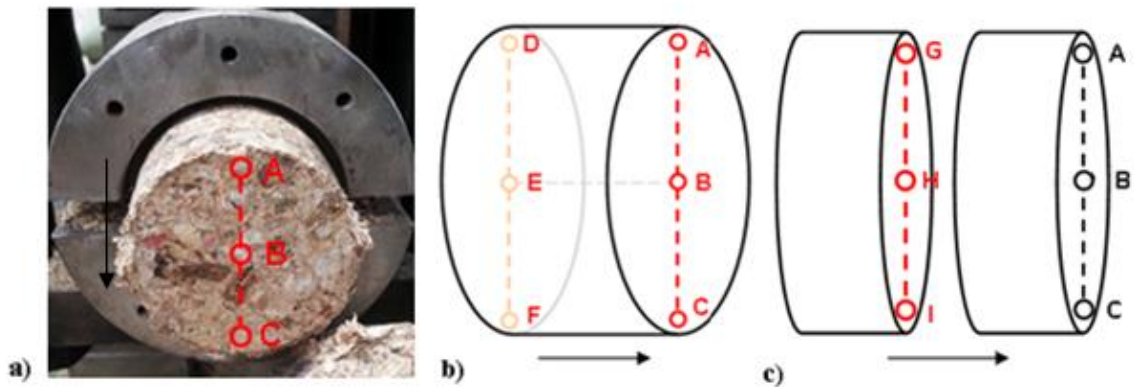
Figure 10: The scheme of scanned points
Source: a) Agico Group, not dated

The taken images were saved in the PC and subsequently analysed through Nis-Elements Advanced Research 2.3, special software for the image processing and data measurement. Before the measurement itself, image calibration using reference object (graph paper) was done – 6.97 $\mu m.px^{-1}$. Then the manual measurements of particles' size in terms of lengths and areas were carried out with the readout 0.01 μm within images. The measurements were done for particles which had clearly defined edges. As already mentioned, the biomass particles have a very irregular shape (Guo *et al.*, 2012), so the procedures of measuring the particle lengths and areas were beforehand defined. Particle's length was measured from one end to the other, approximately halfway through particle along vascular bundles. Particle's area was measured along the outer edges of the particle (Figure 11). The measurements showed the minimum values, not exact, since the particles were not always been displayed on the image in its full dimensions. To compare

behavioural pattern of specified surface locations (i.e. points A, B, C, D, E and F) on briquettes, it was intended to make 10 of these particle measurements for each point within the one briquette, thus 50 measured particle lengths and areas for each point/location. Unfortunately, it was not always possible to make 10 measurements per image, since particles in selected location of scanning have not been clearly defined edges. Therefore, in few cases less than 10 measurements of particles' length and areas within the image and *vice versa* missing measurements were caught in further images, where more than 10 particles were clearly demarcated and so could be measured. However all in all, 50 measurements have been obtained for each scanned point, 300 measurements for all images within the one biomass material (points A, B, C, D, E and F), and totally 900 measurements of particle's lengths and areas for all materials. Images from G, H and I locations were not able to analyse, since there were no clearly defined particles, thus only qualitative assessment was performed. To make qualitative analysis complete, several supporting images of undensified materials were taken as well as some images were subjected to thresholding function to observe dispersion of natural binders.
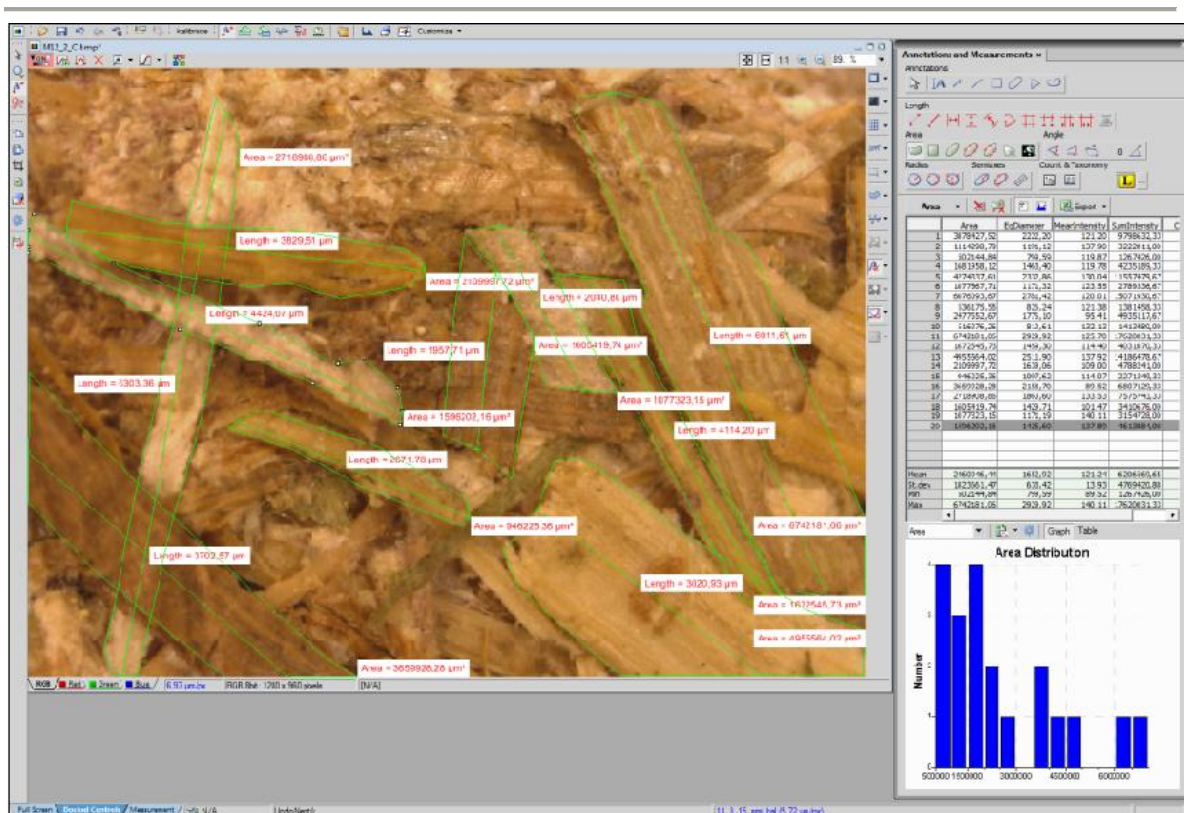
Figure 11: Measurements of lengths and areas of miscanthus particles
Source: Author, 2015

5.2.3 Data processing

The obtained data were processed and statistically analysed using Microsoft Office Excel and/or Statistica 12 software. The data from moisture content and PSD analysis were processed via MS Excel and results were tabulated and/or plotted and discussed.

In case of measurements of lengths and areas, the data were continuously tabulated directly in Nis-Elements program and at the end of analysis the data were imported to MS Excel for cleaning, and then converted to Statistica 12 where the statistical analysis was done. Data were underwent to descriptive statistics analysis – arithmetic means, medians, minimum and maximum values, variance and standard deviation, and statistical hypothesis test for testing of set thesis hypothesis. With respect to the objectives of the thesis and set thesis hypothesis, test ANOVA for comparing the independent samples, i.e. scanned locations on the briquette structure in terms of particles' size, was intended to use. Before statistical hypothesis testing, the data were tested for normality to find if the data are normally distributed. It is an assumption of majority of statistical tests and specifically ANOVA test (Taylor, 2007). In this case, the data were not normally distributed, thus another assumption – homogeneity of variances did not have to be tested. For the statistical testing, non-parametric test was used, i.e. Kruskal-Wallis test (equivalent of the one-way ANOVA), with significance level α 0.05. Obtained results were listed in tables or plotted in graphic form and subsequently discussed.

6 Results and discussion

This chapter provides the findings from the practical research according to the hypothesis and objectives of this thesis and compares it with the relevant findings of other authors. Firstly, results of input parameters of raw materials, moisture content and particle size distribution, which highly affect densification behaviour during briquetting, are presented, followed by main results from macroscopic analysis of produced briquettes.

6.1 Moisture content

The moisture content (MC) of examined ground biomass materials before briquetting process is presented in the Table 1.

Table 1: Moisture content of selected biomass materials

Biomass material	Biomass moisture content (%)
Miscanthus	9.91
Hemp	8.82
Pine sawdust	10.35

As the Table 1 shows, MC values of selected materials are very close to each other and range about arithmetic mean of 9.7%. The lowest MC was found in hemp material, on the contrary, the highest value in pine sawdust. Miao *et al.* (2013) reported MC of *Miscanthus × giganteus* L. before compression 11.5%, Ivanova (2012) 7.28%. In case of pine sawdust, Stolarski and co-workers (2013) determined MC $10.85 \pm 0.02\%$ and Guo *et al.* (2012) 9.3% w.b. For hemp material Ivanova (2012) found MC of 7.31%.

According to the technical norm (ČSN EN ISO 17225-1, 2015) MC of quality solid biofuels should not exceeds 15%. Optimal MC of plant biomass residues meant for combustion differs from study to study. According Chen *et al.* (2009) it should pertain to the range of 10–15%. The same MC range is recommended also by Grover and Mishra (1996) however they stated that the best results are achieved to 12% MC. Demirbas (2004) found that the increasing MC (7–15%) of spruce wood sawdust and pulping reject resulted in stronger briquettes. Li and Liu (2000) found that the ideal MC for wood compactions ranges from 5 to 12%, and recommend optimal content 8%. Based on Kaliyan's and Morey's study (2009) MC of feedstock should be of 12–20%, since it can help the binding

mechanisms during densification process under room temperature. Kers *et al.* (2010) determined optimal material MC to the interval 10–18%. According to Mani *et al.* (2006b) low MC of corn stover (5–10%) results in denser, more stable and more durable briquettes than high moisture stover (15%). Generally, the critical MC for safe storage of biomass is less than 15% (Kaliyan, 2008). On the other hand, Wamukonya and Jenkins (1995) produced briquettes made of agricultural residues and wood wastes of good quality, which content of moisture ranged of 12 to 20% (w.b.).

It can be concluded that generally MC of biomass material before densification should not exceed 15% and how these results showed, the studied materials belongs to this recommended and normatively set boundary.

6.2   Particle size distribution analysis

Particle size and its distribution is one of the most important factors affecting physical properties of briquettes (Zhang and Guo, 2014). Since it defines agglomerative behaviour during briquetting process (Pietsch, 2002), the particle size distribution (PSD) analysis of examined materials, using oscillating screen method with sieve apertures of 10 mm and lower, was done within practical research and the results are as follows:

Hemp

Average PSD of hemp is shown in Figure 12. As we can see, more than half of the material was captured on the sieve with largest opening size (i.e. 10 mm). It is due to the
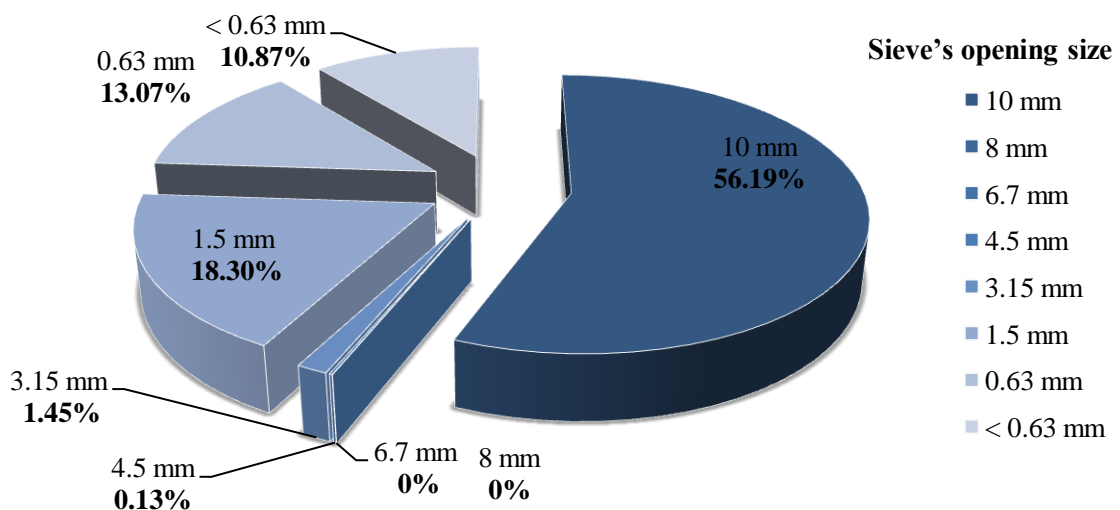
Figure 12: Pie chart of particle size distribution of hemp material

fibrous nature of hemp; long hemp bast fibres did not be ground well and created tangled masses, which could not fail through openings and thus stayed on the first sieve. In both tests, following sieves (opening sizes 8 and 6.7 mm, respectively) did not catch any material. Almost all the rest of the non-fibre part of stem and leaf tissues, i.e. epidermis, cortex, phloem, xylem, and mainly pith, passed through sieves (however some of them were caught and tangled by bast fibres on the first sieve) and the sieve with opening size 1.5 mm captured the most of these non-fibre based particles, followed by sieve with aperture 0.63 mm and bottom pan (< 0.63 mm).

Figure 13: Particle size distribution of hemp

Notices: particles retained on the sieve with the largest aperture on the right,
with the smallest aperture on the left side; sieves with no captured material (8 and 6.7 mm) were omitted

As is evident from Figure 13, due to the fibrous nature, sieve-based analysis of hemp did not yield absolutely reliable results on real PSD; however it had provided the helpful information about structural composition of the material, which was used for subsequent macroscopic analysis of briquettes.

Miscanthus

PSD of Miscanthus material is presented in the pie chart in Figure 14. It is obvious, that minimum of material was captured by the sieves with largest opening sizes (10, 8 and 6.7 mm). As well as following sieves (4.5 and 3.15 mm) caught the small part of the mass (about 5%). On the other hand, more than 50% of the miscanthus material was retained on sieve with aperture 1.5 mm. Followed by the last sieve and bottom pan which captured together the rest of the material (approximately 44%).
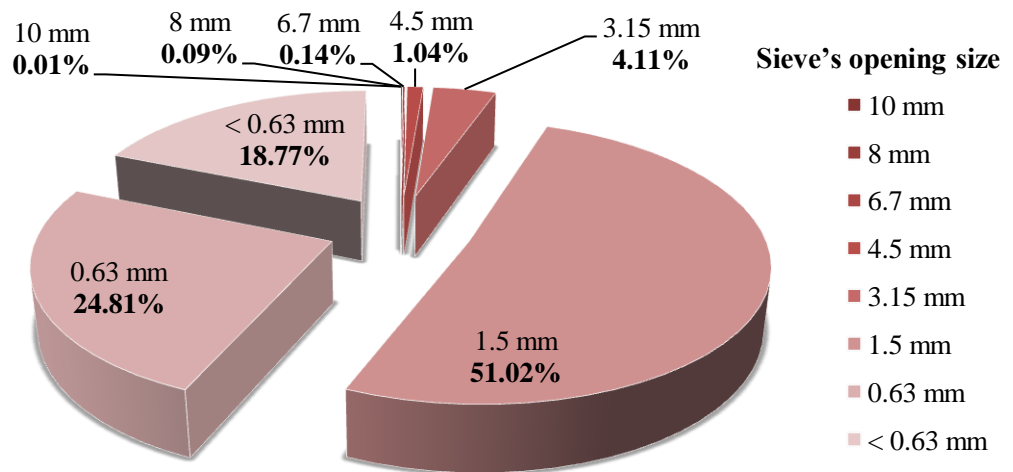
Figure 14: Pie chart of particle size distribution of miscanthus material

Although the largest screens (10, 8, 6.7, 4.5 mm) captured minimum of miscanthus material (less than 1.3%), from visual assessments, it is evident that lengths of many particles exceeds the largest sieve opening size and that the lengths of particles captured on the sieves did not correspond with opening size of the screens. As was stated, more than 50% of the miscanthus material was retained on sieve with aperture 1.5 mm, i.e. the size of particles should be less than 3.15 mm and more than 1.5 mm, however it does not reflect real size of particles as can be seen in Figure 15.

Figure 15: Particle size distribution of miscanthus

Notice: particles retained on the sieve with the largest aperture are on the right,
with the smallest aperture are on the left side

It indicates that the mechanical screening procedure did not determine the real sizes of miscanthus particles well due to their needle-like shape. This method was already previously presented as to be not obviating the "falling-through" effect of longer particles through smaller apertures on sieve (Igathinathane *et al.*, 2009a). Several studies shown sieve analysis based approach for PSD, notwithstanding it is considered as a standard testing procedure (ČSN EN 15149-1, 2011), as not precise method of classifying the particulate materials by length (Womac *et al.*, 2007; Igathinathane *et al.*, 2009a; Igathinathane *et al.*, 2009b).

Pine sawdust

The distribution of pine sawdust particles was more uniform than that of previous materials, as can be seen in Figure 16 and pie chart of Figure 17. Owing to the spherical shape of pine sawdust particles, decreased screen opening size resulted in really decreased particle sizes, as expected.

Figure 16: Particle size distribution of pine sawdust

Notice: particles retained on the sieve with the largest aperture are on the right,
with the smallest aperture are on the left side

More than 60% of the material was captured by last three sieves and bottom pan (with apertures 3.15, 1.5, 0.63 and <0.63 mm respectively). The largest mass (almost 25%) was captured on the sieve with aperture 1.5 mm. On the contrary, the screens with the largest apertures (10, 8, 6.7 mm) caught the least amount of material due to the spherical shape of sawdust particles, the standard oscillating method determined reliable results of more or less the real sizes of sawdust particles, as can be seen in Figure 17.
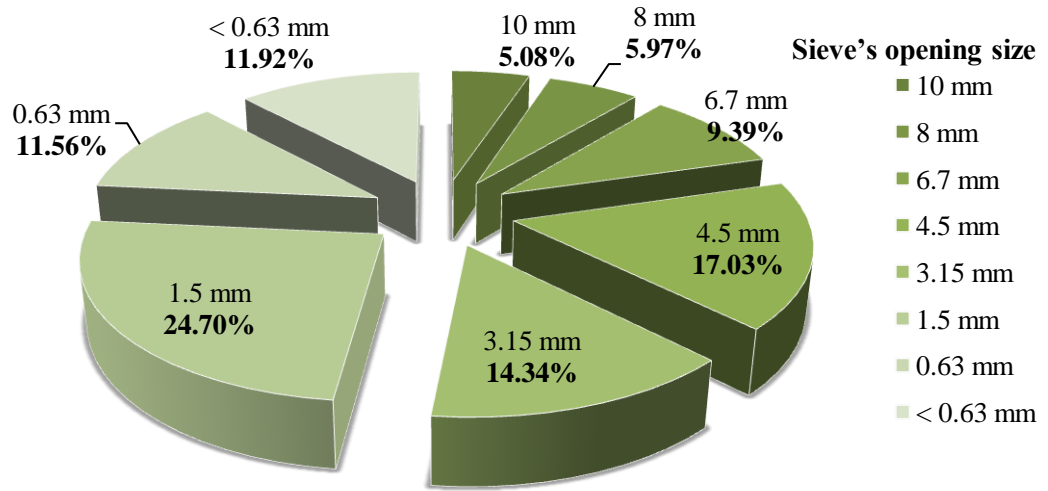
Figure 17: Pie chart of size distribution of pine sawdust particles

To compare the PSD of all three studied materials, the results were collectively tabulated and plotted. Following Table (2) shows arithmetic means and percentage of materials retained on individual sieves and bottom pan, as well as the initial mass which was poured into the top sieve with the largest screen openings at the beginning of the PSD analysis. The graphical comparison of the individual materials you can see as well in line chart in Figure 18.

Table 2: Particle size distribution of examined materials

	Material retained on sieve					
Sieve	*Miscanthus*		*Hemp*		*Pine sawdust*	
(mm)	**(g)**	**%**	**(g)**	**%**	**(g)**	**%**
10	0.01	0.01	23.11	56.19	4.22	5.08
8	0.06	0.09	0	0	4.96	5.97
6.7	0.10	0.14	0	0	7.79	9.39
4.5	0.69	1.04	0.06	0.13	14.14	17.03
3.15	2.73	4.11	0.60	1.45	11.90	14.34
1.5	33.80	51.02	7.53	18.30	20.50	24.70
0.63	16.44	24.81	5.38	13.07	9.59	11.56
< 0.63	12.44	18.77	4.47	10.87	9.90	11.92
Total	66.25	100	41.13	100	82.98	100
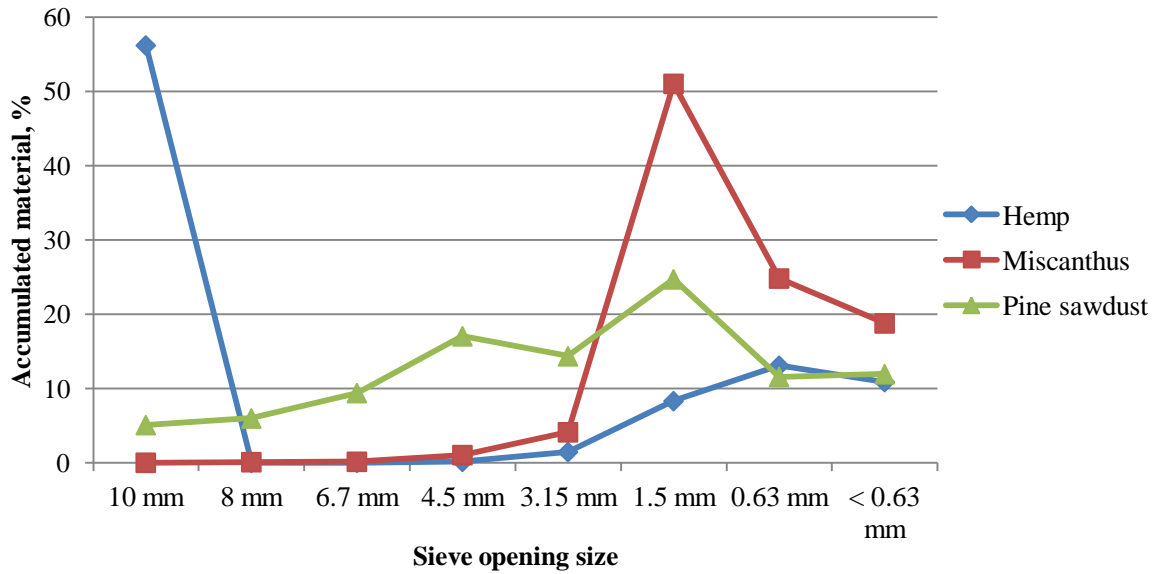
Figure 18: Comparison of particle size distributions of examined materials

6.3   Dimensions of produced briquettes

The briquettes were produced from selected materials: perspective perennial energy plant – miscanthus, interesting annual fibre plant – hemp, and traditional representative of biofuel material – pine sawdust. The produced briquettes from each examined biomass material you can see in Figure 19 on the next page. The lengths and diameters of examined briquettes show Table 3.

Table 3: The length and diameter of selected briquettes

No. of briquette	Hemp		Miscanthus		Pine sawdust	
	Length (mm)	Diameter (mm)	Length (mm)	Diameter (mm)	Length (mm)	Diameter (mm)
1	30.28	66.54	48.13	68.38	46.32	68.09
2	34.09	66.92	53.91	69.55	48.92	67.77
3	43.37	66.73	49.33	68.97	43.07	67.81
4	40.06	67.02	45.87	68.54	44.60	67.76
5	33.26	67.07	37.83	68.34	48.20	67.78
Arithmetic mean	**36.21**	**66.86**	**47.01**	**68.76**	**46.22**	**67.84**

As is evident from the Table 3, the briquettes made of miscanthus had the largest length and diameter. On the contrary, the briquettes from hemp had the smallest dimensions. It is evident, that all briquettes had larger dimensions than dimensions defined by stamping die of briquetting press, i.e. with matrix diameter 65 mm. It is due to fact that deformation and densification in case of biomass material are not permanent and elastic spring back occurs after pressure release (Pietsch, 2002). The diameter of briquettes made of hemp was the closest to the die diameter. On the contrary, miscanthus briquettes had the most distant diameter value from the matrix diameter. With the same type of briquetting press, similar results (i.e. briquette diameter is larger than the die diameter) were obtained by Brožek *et al.* (2012) with the briquettes made of following materials: birch chips, poplar chips, pine bark, spine sawdust and spruce shavings. They calculated relatively close dependence between the briquettes density and their diameter (d = $-0.013 \times \rho + 77.68$; R^2 = 0.95). From this dependence, it is evident that briquettes with higher density raise their diameter less than the briquettes with lower density. Based on visual assessment and manipulation, this dependence could be assumed also in our case, since the miscanthus briquettes having the largest diameter evinced characteristics of the lowest density and mechanical durability.

Figure 19: Produced briquettes made of different biomass sources
Notice: a) hemp, b) miscanthus, c) pine sawdust

6.1 Macroscopic analysis

6.1.1 Qualitative analysis

In total, 135 colour 2D images of briquettes' cross-sectional surface structure were obtained, i.e. 45 images for each biomass material. In Figure 20, images of briquette structure at particular scanned point for all three materials, are presented.

Biomass material			
Point	Hemp	Miscanthus	Pine sawdust
A			
B			
C			
D			
E			

Figure 20: Scanned images (magnification 6.5×) of cross-sections at defined points

Notice: the briquettes no. 2 are presented

The outputs of the complex compaction process can be observed in the selected locations (points) of the observed briquettes' surfaces (Figure 20). Process of the structure alteration of the input material was dependent and inseparable associated with the process of pressing agglomeration, i.e. pressing of the loose feedstock materials of hemp, miscanthus and pine sawdust in the pressing chamber of the briquetting machine BrikStar CS 50 during which external forces acted on the mass of particles. The process of briquette compaction was accompanied by a change in the state of the original material with loose particles, as can be evident from the comparisons of Figure 21, where the ground materials before densification (the images are taken with the same magnification 6.5× as in case of all images of briquette structure) are presented, and already mentioned Figure 20 with the densified compacts' surface structures.

Figure 21: Undensified materials before briquetting

Notices: a) hemp, b) miscanthus, c) pine sawdust;
Magnification 6.5×

In the initial phase, discrete particles did not have a definite and uniform formation (as evident form Figure 21); gradually particle rearrangement took place owing to application of low pressure to break down the unstable packing arrangement of particles. Later, elastic and plastic deformation of particles occurred during application of high pressure, when particles' passed through the pre-chamber and the matrix, which led to particles' flow into empty spaces, removal of the air and increased contact among particles. The particles of the original input materials, mainly fibres of hemp, flat-shaped of pine sawdust and elongated of miscanthus as well as other irregularly shaped particles, were weaved, twisted, and bended about each other and deformed during compaction which led to mechanical interlocking bonds between these particles. This process is clearly obvious from the images of inner surface, i.e. points G, H and I (Figure 20). Kaliyan and Morey (2010) studied mechanical interlocking of corn stower and switchgrass particles via light microscopy with similar results.

In our case, where no binding agents for increase the briquette strength were used, binding and adhesion of particular particles in the briquette pressing chamber occurred owing to secretion and activation of natural binders, at high compression pressures of approximately 18 MPa and temperatures reaching about 60°C (Briklis, not dated), during densification which acted as local binders of particles. After densification process, when pressure and temperature were ceased, the natural binders hardened and formed bonds or bridges between particles. This mechanism affords high density and strength of the produced briquettes without lacking of binding agents' addition (Muntean *et al.*, 2012; Ivanova, 2012). As was mentioned (subchapter 2.6.1.2) the biomass materials contain, in various amounts, natural binders, such as water soluble carbohydrates, lignin, cellulose,

protein, starch and fats (Back 1987; Kaliyan, 2008; Chou *et al.*, 2009; Kaliyan and Morey, 2010). In case of pine sawdust, bonding at lignin and cellulose surface areas was most probably accountable for the major kind of bonding mechanism in the press-drying process (Back, 1987). These secreted natural binders can be observed as transparent natural resin coats on the densified particles as you can see in Figure 22. This process was observed also by Kaliyan and Morey (2010) in case of corn stower and switchgrass briquettes. They found, with using fluorescence microscopy, that solid bridges were formed primarily by lignin and protein. Muntean *et al.* (2012) in their study also detected lignin secretion by image analysis in case of briquettes made of mixtures of grapevine, straw and corn stalks.

Figure 22: Typical glassy coating of natural binders on biomass particles
Notice: miscanthus briquette no. 3 at point B with magnification 6.5×

Figure 23 presents distribution of secreted natural binders and especially lignin (as studies' findings shows) on hemp briquettes' surface via tresholding function that highlighted in red colour areas of glassy coating. As can be seen the distribution of the binders is focused primarily on non-fibre part of stem and leaf tissues – mainly pith, whereas the bast fibres show no secretion. According to Gutiérrez *et al.* (2006) it is caused by low content of lignin in bast fibres of industrial hemp, which accounts for 4.6% of the total fibre. More precise results could be obtained using UV-fluorescence microscopy to detect natural binders, which generate blue fluorescence for lignin and yellow-green for protein compounds (Rost, 1995). Such method was used by already mentioned Kaliyan and Morey (2010) in their studying of corn stower and switchgrass briquettes. As well as chemical analysis could provide information about amounts and share of these compounds.
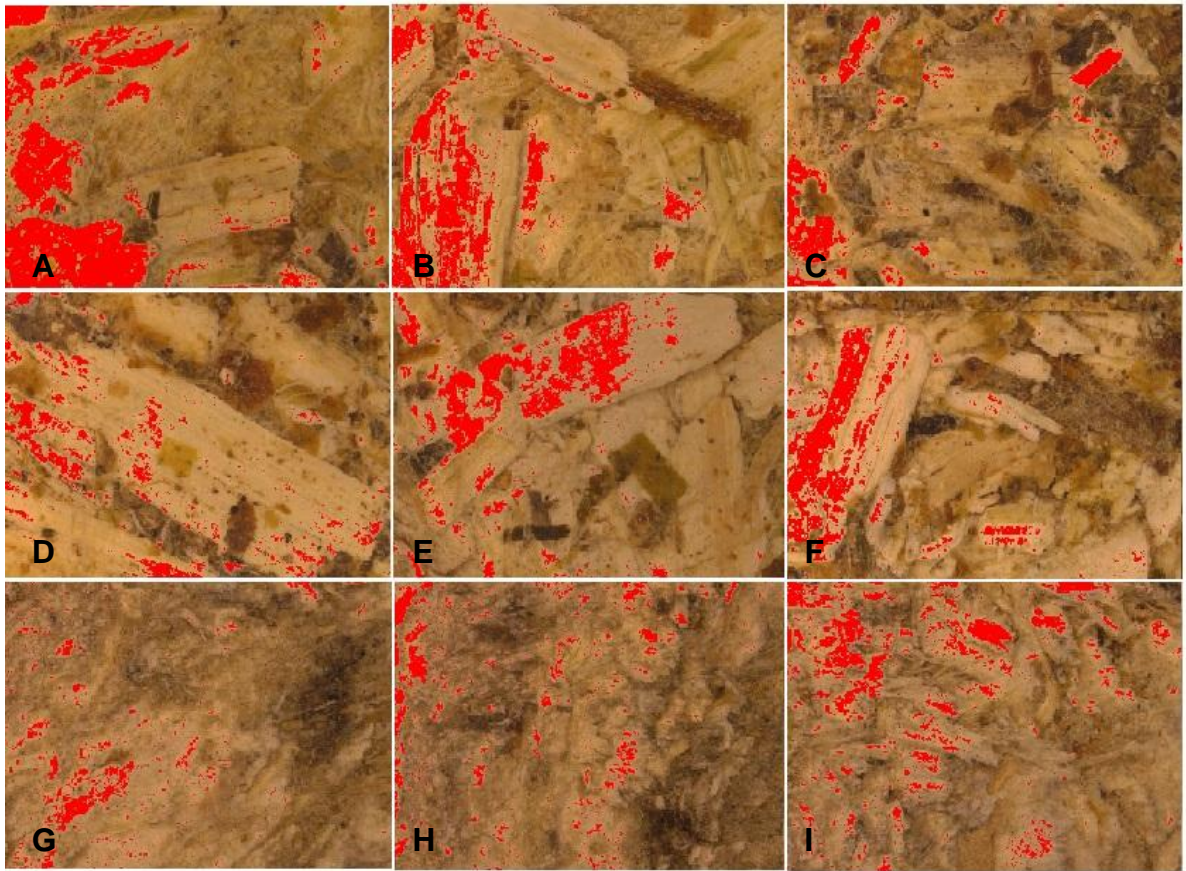
Figure 23: Natural binders' detection using tresholding function

Notices: all points on hemp briquette, no. 3, are presented;
magnification 6.5×

Solid bridges, one of the binding mechanisms (Rumpf, 1962; Pietsch, 2002), were formed by hardening of bonding agents, i.e. natural binders and mainly lignin as we can assume. From the images, formation of these solid bridges we can observed primarily in case of surfaces of the rear part of the briquettes (points D, E, F) and inner surfaces, i.e. locality of points G, H and I. As is evident from Figure 20 and 24, the rear part of the briquettes (where the points D, E, F were located) is characterized by the stronger upper layer, the high level compaction and deformation of the original raw material particles, owing to the direct action of the piston in pressing chamber to the mass of the compacting material (Figure 25). These binging and compaction mechanisms were also reported by Kaliyan and Morey (2010) and Ivanova (2012).
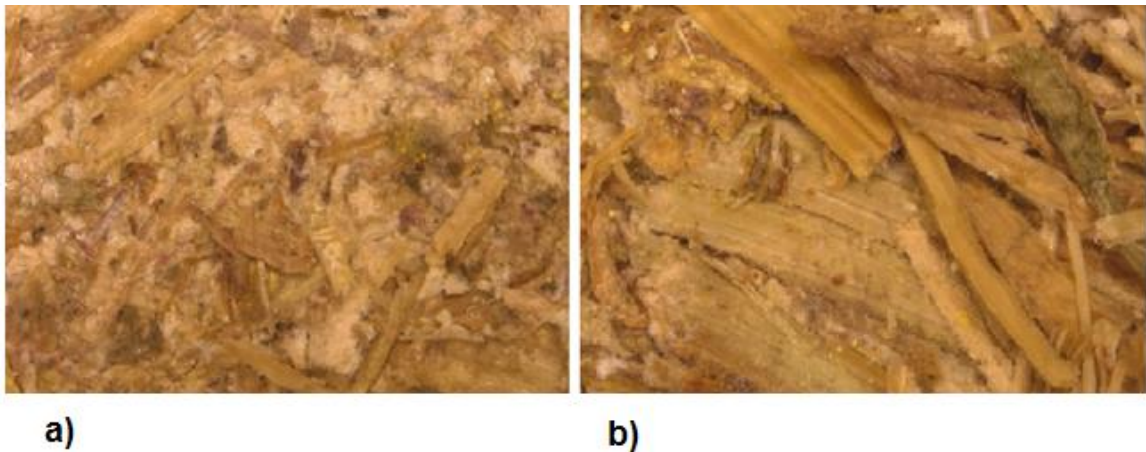
Figure 24: Comparison of briquette sides
Notices: a) stronger upper layer of rear side (point F), b) the front side of the briquette (point C); Miscanthus briquette no. 3

The solid bridge can be also activated by moisture (Pietsch, 2002). Water as moisture in biomass feedstock serves as important agent that plays role of binder and lubricant (Kaliyan and Morey, 2010), since water supports development of bonding by van der Waals' forces by increasing the contact area between particles (Grover and Mishra, 1996; Pietsch, 2002). Pickard *et al*. (1961) reported that the degree of adhesion increased with increasing MC in lucerne hay. In our case, the MC values of studied materials (with arithmetic mean 9.69%) belongs to the recommended and normative boundary of 15% which along with applied heat (60°C) allowed activation of various physical and chemical processes enabling compressibility of particles. The formation of solid bridges is obvious from the Figure 25, where images with 50× magnification are presented.
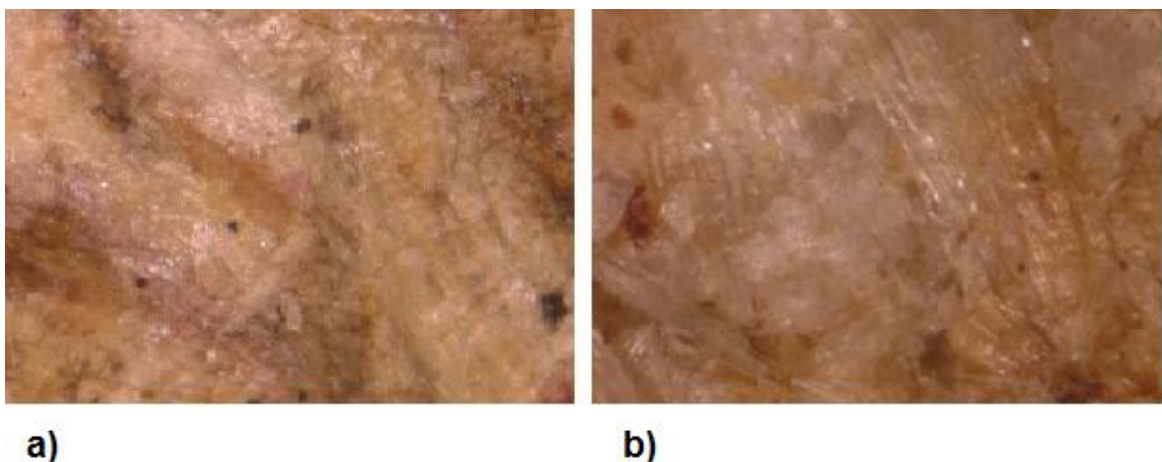
Figure 25: Surface of pine sawdust briquette with magnification 50×
Notice: a) Miscanthus briquette no. 1, point D, b) pine sawdust briquette no. 1, point D

51

The effectiveness of these binding mechanisms, i.e. adhesion and bonding between surfaces of input particles in terms of interlocking bonds and solid bridges, was affected, besides others, by structural and chemical composition of material, particle size and shape, particle roughness, presence of irregularly shaped particles, like hemp fibres and elongated miscanthus particles, and presence of air cavities and pores (Muntean *et al.*, 2013).

Generally, particle morphology is quite different for all three bio-materials, however it is related to initial particle morphology which was more or less retained, as can be seen form Figures 20 and 21. As can be seen, the particles of miscanthus are the longest, which also corresponds with the results of PSD analysis; miscanthus surface structure also exhibits the highest porosity. This higher porosity may indicate decreased density of the briquette (Zhang and Guo, 2014). Smaller particles can be observed on hemp briquettes. It is evident, that the characteristic properties of the briquette surface locations are similar for all briquettes made of different biomass sources. Generally, larger particles are located on the front side of the briquettes (i.e. points A, B and C), whereas smaller are situated on the rear side (D, E and F). Particle morphology under application of pressure also underwent several deformations and fractions, especially in case of miscanthus which larger particles were disintegrated.

As evident from Figure 20 the particles on the surface have only an imperceptible uniform and regular orientation and distribution, in their agglomeration is no obvious pattern. Only in case of the inner surfaces, there could be evident the similar particle orientation, however it is due to cutting by electric band saw, when the particles were deformed and arranged according to the direction of cut (and thus particles on inner surface – points G, H, I could not be measured). It is evident that the particles lying on the surface of the briquettes are oriented along the cross-sections and *vice versa* particles inside the briquettes (inner surface) are mostly oriented perpendicular to the cross-section – it also partly caused that particles on inner surface could not be measured.

Altogether, we can say that all scanned points of the briquette surface or better said behavioural pattern of the material at each scanned point have its different attributes which can be explicated by the demeanour of the material mass going through the pressing chamber of the piston briquetting press BrikStar. It is obvious that the agglomeration and compaction of particles occurred unequally in different zones of the briquette surface and zones of interaction of pressed material with piston of briquetting machine.

6.1.2 *Quantitative analysis*

6.1.2.1 *Descriptive statistics of measured values*

By measuring particles' size in terms of lengths and areas within 90 scanned images of briquette surface (points A, B, C, D, E, and F) 900 values of lengths and areas were obtained. Table 4 shows descriptive statistics of measured values of length and areas according to the biomass source of the briquettes.

Table 4: Descriptive statistics of examined materials (in mm/mm^2)

		N	*Mean*	*Median*	*Min*	*Max*	*Std. Dev.*	*Variance*
Hemp	*Area*	300	2.86	1.70	0.08	22.98	3.11	9.69E+06
	Length	300	2.60	2.16	0.54	9.48	1.60	2.55E+03
Miscanthus	*Area*	300	2.89	1.67	0.10	25.62	3.44	1.18E+07
	Length	300	3.33	2.82	0.46	9.04	2.04	4.18E+03
Pine sawdust	*Area*	300	2.16	1.11	0.04	17.08	2.69	7.25E+06
	Length	300	1.77	1.39	0.27	6.34	1.22	1.49E+03

Notice: E notation in Variance values means 10^x – e.g. in case of $9.69E+06 = 9.69 \times 10^6$

As can be seen in the Table 4, according to values of arithmetic mean, miscanthus particles are the largest, which corresponds to the visual assessment from previous subchapter. However the smallest particles are evinced by pine sawdust, not hemp as was thought. Although PSD analysis of undensified materials showed that the particles were often larger than the size of fraction (12 mm), here maximum values of length did not exceed 10 mm. It could be caused by particles' fractions during pressure application in pressing chamber or just the fact, that the real dimensions of particles could not be measured owing to their sizes exceeding size of image. We can also see that variance is quite high, which indicates that the measured values are very spread out around the mean and from each other. It is due to the fact that grinded particles have wide size range, as shown PSD analysis. This is also linked to the median value, which is relatively far from the mean.

The Table 5 on next page shows descriptive statistics of the obtained data (in mm/mm^2) divided according to scanning locations. The overall tables with all measured data (in μm/ μm^2) are presented in annex (Tables I-III).

Table 5: Descriptive statistics of studied points on briquettes' surface (in mm/mm^2)

		N	Mean	Median	Min	Max	Std. Dev	Variance
A	*Area*	150	3.15	1.89	0.18	14.34	3.00	9.02E+06
	Length	150	2.75	2.39	0.58	8.72	1.71	2927.18
B	*Area*	150	3.63	2.55	0.08	25.62	3.66	1.34E+07
	Length	150	3.09	2.60	0.57	8.69	1.77	3.12E+03
C	*Area*	150	2.42	1.60	0.13	14.43	2.45	6.02E+06
	Length	150	2.59	2.06	0.57	8.91	1.75	3.05E+03
D	*Area*	150	2.20	1.04	0.04	22.98	3.45	1.19E+07
	Length	150	2.38	1.68	0.27	9.48	1.90	3.61E+03
E	*Area*	150	2.82	1.41	0.08	22.05	3.30	1.09E+07
	Length	150	2.59	1.99	0.30	9.04	1.88	3.53E+03
F	*Area*	150	1.59	0.77	0.08	14.39	2.11	4.47E+06
	Length	150	2.01	1.44	0.37	6.76	1.44	2.07E+03

Notice: E notation in Variance values means 10^x – e.g. in case of $9.02E+06 = 9.02 \times 10^6$

From values of mean and median it is evident, that the front side of the briquettes (points A, B, C) contains larger particles. Again we can see relatively high variances, which indicates that the measured data within set points are very spread out around the mean and from each other. These results indicate that the measured data did not come from a normal distribution.

6.1.2.2 Thesis hypothesis testing

Based on the set hypothesis analysis of the distribution of particles' sizes within the set points on the briquettes' surface was done and for its verification following statistical methods were used.

Before the application of the intended statistical testing, the data were checked (based on the outputs of descriptive statistics) for the normality via Kolmogorov-Smirnov, Lilliefors and Shapiro-Wilk's tests. As can be seen from the results of normality tests within the Table 6, p-values were lower than set significance level 0.05, thus we rejected the null hypothesis[7] that the data have normal distribution and accepted alternative hypothesis. For this reason, to compare particles' sizes within points, non-parametric test, i.e. Kruskal-Wallis test[8], was used for our proving of thesis hypothesis.

---

[7] Null hypothesis – data are sampled from a Gaussian distribution, alternative hypothesis – data are not sampled from a Gaussian distribution.

[8] Even though a non-parametric tests are less powerful than the parametric ones (Taylor, 2007), in this case, as is presented in next page, the test provided results with more than 99% confidence level.

Table 6: Tests of normality for groups of points (A, B, C, D, E, F)

Tests of normality			*max D*	*K-S p*	*Lilliefors p*	*W*	*p*
Group	*Variable*	*N*					
A	*Area*	150	0.185442	**p < 0.01**	**p < 0.01**	0.833194	**0.000000**
	Length	150	0.125855	**p < 0.05**	**p < 0.01**	0.873075	**0.000000**
B	*Area*	150	0.178761	**p < 0.01**	**p < 0.01**	0.757597	**0.000000**
	Length	150	0.131305	**p < 0.05**	**p < 0.01**	0.915780	**0.000000**
C	*Area*	150	0.190992	**p < 0.01**	**p < 0.01**	0.784472	**0.000000**
	Length	150	0.133917	**p < 0.01**	**p < 0.01**	0.873344	**0.000000**
D	*Area*	150	0.266239	**p < 0.01**	**p < 0.01**	0.599714	**0.000000**
	Length	150	0.162666	**p < 0.01**	**p < 0.01**	0.854620	**0.000000**
E	*Area*	150	0.203687	**p < 0.01**	**p < 0.01**	0.739761	**0.000000**
	Length	150	0.136488	**p < 0.01**	**p < 0.01**	0.887695	**0.000000**
F	*Area*	150	0.237476	**p < 0.01**	**p < 0.01**	0.675745	**0.000000**
	Length	150	0.168584	**p < 0.01**	**p < 0.01**	0.852398	**0.000000**

Notices: K-S – Kolmogorov-Smirnov test, W – Shapiro-Wilk's test

The outputs from Kruskal-Wallis test, the non-parametric equivalent of the one-way ANOVA, for **length variable** is presented in Table 7.

Table 7: Kruskal-Wallis test for length variable

Dependent Length	*Code*	*N*	*Sum of Ranks*	*Mean Rank*
A	1	150	74122.00	494.1467
B	2	150	81877.50	545.8500
C	3	150	68477.00	456.5133
D	4	150	60374.00	402.4933
E	5	150	66472.50	443.1500
F	6	150	54127.00	360.8467

Kruskal-Wallis ANOVA by Ranks
Independent (grouping) variable: Point
Kruskal-Wallis test:
H (5, N = 900) = 47.56759 **p = 0.0000**

Based on the achieved significance level Kruskal-Wallis test (p ≐ 0.0000), we can declare that we have demonstrated a statistically significant difference (with more than 99% confidence) in lengths of specified points[9]. From the sum of the ranks for the particular groups is evident that the lengths of particles are the largest at the point B,

---

[9] Based on the fact that the p-value is lower than set significance level (0.05), we rejected the null hypothesis that the length (or area) data are equal in terms of medians, and thus alternative hypothesis, that at least two of the medians are different, was accepted.

followed by points A, C, E, D, and F. In general, larger particles were located on the front side, contrarily the smaller ones were found on the rear side of the briquettes. The same results, graphically expressed through box plots, can be seen at the Figure 26.
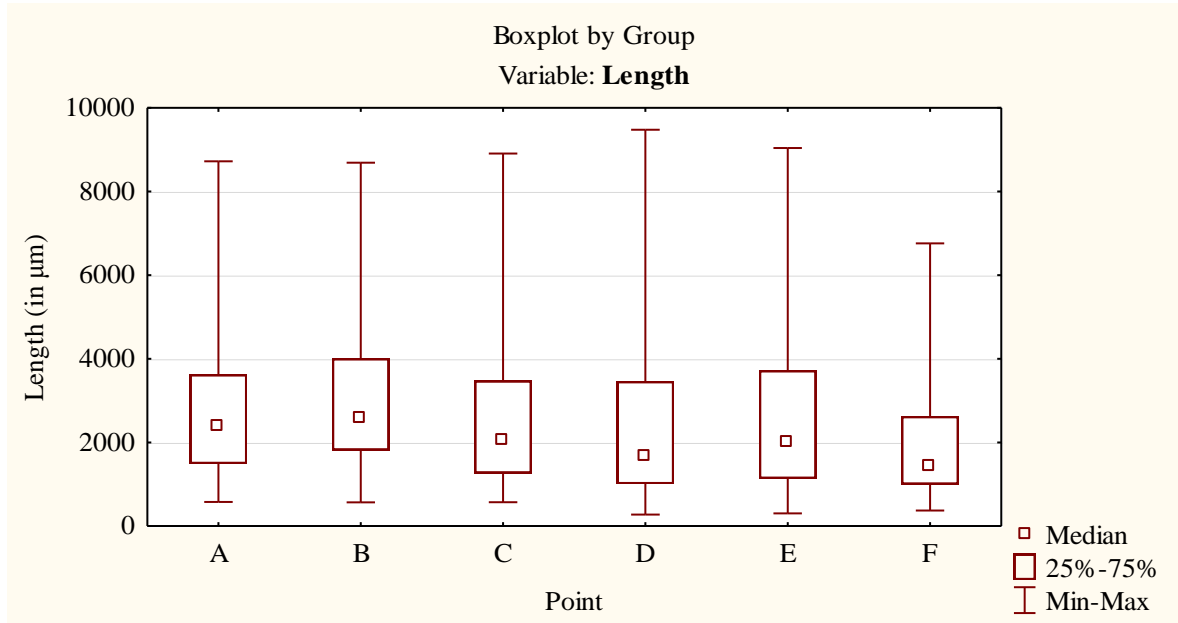
Figure 26: Group box plot for length variable (in µm)

Table 8 presents the results from Kruskal-Wallis test for **area variable.**

Table 8: Kruskal-Wallis test for area variable

Dependent Area	*Code*	*N*	*Sum of Ranks*	*Mean Rank*
A	1	150	77625.00	517.5000
B	2	150	84355.00	562.3667
C	3	150	69373.00	462.4867
D	4	150	55087.00	367.2467
E	5	150	69595.00	463.9667
F	6	150	49415.00	329.4333
Kruskal-Wallis ANOVA by Ranks Independent (grouping) variable: Point Kruskal-Wallis test: $H (5, N = 900) = 86.38499$ **p = 0.0000**				

We may also assert in case of area variable that we have demonstrated a statistically significant difference (with more than 99% confidence) among measured values in specified zones (points), based on the achieved significance level of Kruskal-Wallis test ($p \doteq 0.0000$). From the sum of the ranks for the particular groups (points) is evident that the

areas of particles are the largest at the point B, followed by points A, E, C, D, and F. The same results, graphically expressed in box plots, can be seen at the Figure 27 as well.
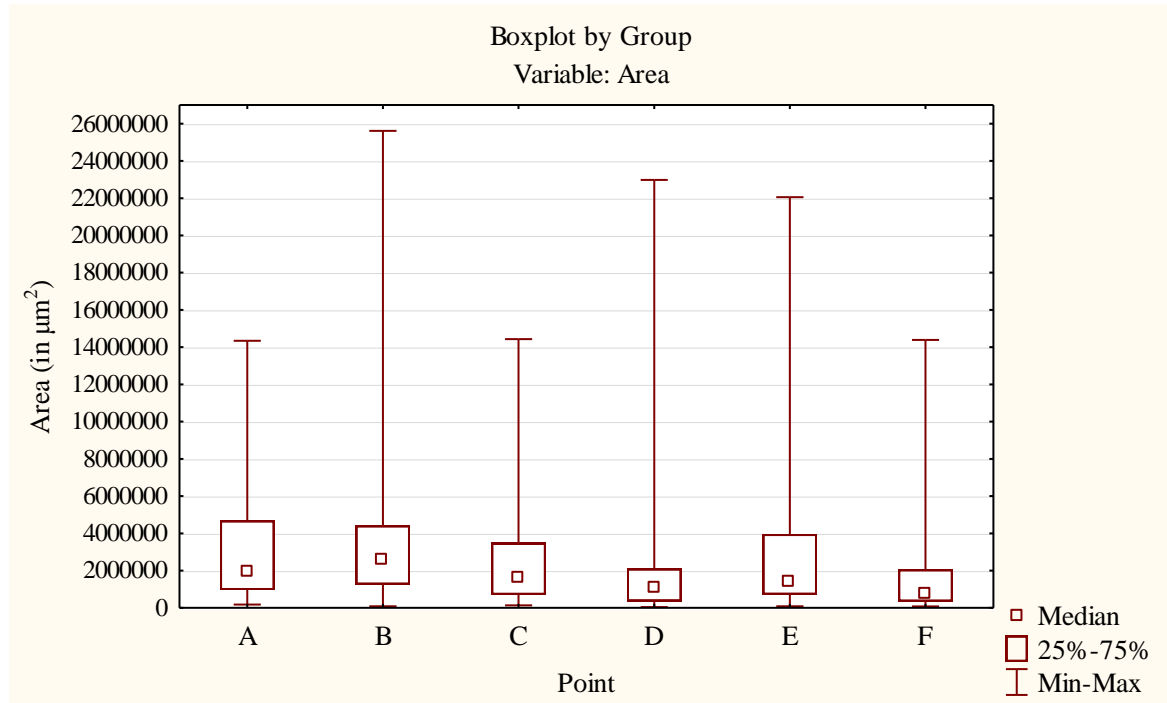
Figure 27: Group box plot for area variable (in µm^2)

To make testing complete, multiple comparisons tests were done and following Tables (9-12) show where the significant differences (highlighted by red colour) between the scanned points occur. The Tables 9 and 11 show z values (standard scores) for each comparison between points. Tables 10 and 12 show p-values associated with each comparison.

Table 9: Multiple comparisons z' values of area values for point variable

Dependent Area	**A** R: 517.50	**B** R: 562.37	**C** R:462.49	**D** R:367.25	**E** R:463.97	**F** R:329.43
A		1.494725	1.832760	5.005664	1.783454	6.265409
B	1.494725		3.327485	6.500390	3.278179	7.760134
C	1.832760	3.327485		3.172904	0.049306	4.432649
D	5.005664	6.500390	3.172904		3.222210	1.259745
E	1.783454	3.278179	0.049306	3.222210		4.481955
F	6.265409	7.760134	4.432649	1.259745	4.481955	

Multiple Comparisons z' values; Area
Independent (grouping) variable: Point
Kruskal-Wallis test: H (5, N = 900) = 86.38499, p = 0.0000

Table 10: Multiple comparisons p values of area values for point variable

Dependent Area	A R:517.50	B R: 562.37	C R:462.49	D R:367.25	E R:463.97	F R:329.43
A		1.000000	1.000000	0.000008	1.000000	0.000000
B	1.000000		0.013145	0.000000	0.015672	0.000000
C	1.000000	0.013145		0.022638	1.000000	0.000140
D	0.000008	0.000000	0.022638		0.019081	1.000000
E	1.000000	0.015672	1.000000	0.019081		0.000111
F	0.000000	0.000000	0.000140	1.000000	0.000111	

Multiple Comparisons p values (2-tailed); Area
Independent (grouping) variable: Point
Kruskal-Wallis test: H (5, N = 900) = 86.38499, p = 0.0000

On the basis of multiple comparisons and set significance level of 0.05, we proved, that there is significant difference in areas mainly between points A and F, which was obvious from the previous testing. Further, there is significant difference primarily between B and F, B and D. It is also evident that there are significant differences in areas between points on the front and their opposite on the rear side of briquettes, i.e. between the point A and its opposite on the other briquette side point D. The same observation is applied for the points B and E, C and F.

Table 11: Multiple comparisons z' values of length values for point variable

Dependent Length	A R:494.15	B R: 545.85	C R: 456.51	D R: 402.49	E R: 443.15	F R:360.85
A		1.722488	1.253748	3.053415	1.698945	4.440867
B	1.722488		2.976236	4.775903	3.421433	6.163355
C	1.253748	2.976236		1.799667	0.445197	3,187119
D	3.053415	4.775903	1.799667		1.354470	1.387452
E	1.698945	3.421433	0.445197	1.354470		2.741922
F	4.440867	6.163355	3.187119	1.387452	2.741922	

Multiple Comparisons z' values; Length
Independent (grouping) variable: Point
Kruskal-Wallis test: H (5, N = 900) = 47.56759, p = 0.0000

As table on the next page shows, on the basis of multiple comparisons and set significance level of 0.05, we proved, that there is significant difference also in particles' lengths mainly between points B and F, further between B and D. It is also evident that there is no significant difference between points on the front side (i.e. A and B, B and C, C and A) as well as points on the rear side (which means D and E, E and F, D and F).

Table 12: Multiple comparisons p values of length values for point variable

Dependent Length	A R: 494.15	B R:545.85	C R:456.51	D R:402.49	E R:443.15	F R: 360.85
A		1.000000	1.000000	0.033938	1.000000	0.000134
B	1.000000		0.043772	0.000027	0.009344	0.000000
C	1.000000	0.043772		1.000000	1.000000	0.021555
D	0.033938	0.000027	1.000000		1.000000	1.000000
E	1.000000	0.009344	1.000000	1.000000		0.091621
F	0.000134	0.000000	0.021555	1.000000	0.091621	

Multiple Comparisons p values (2-tailed); Length
Independent (grouping) variable: Point
Kruskal-Wallis test: H (5, N = 900) = 47.56759 , p = 0.0000

As it seems from the results of the analysis, we can conclude that particle size distribution on the briquette cross-section surface is not uniform; there are differences between the particle sizes in terms of length and area on the briquette surface. Generally, the largest particles are on the front side, while the particles with smaller dimension are on the rear side.

As was stated before, size of particles significantly affects the physical properties of briquettes (Zhang and Guo, 2014). Particle size as well as particle size distribution play important roles in compressibility of bulk input material and durability of final briquettes (Grover and Mishra, 1996; Ganesan *et al.*, 2008; Kaliyan and Morey, 2009). Generally, reduced particle size leads to increasing density, durability, impact resistance and decreasing compressive strength (Zhang and Guo, 2014), however fine grinding is undesirable due to increased cost of production (Kaliyan and Morey, 2009).

Based on the searching and studying of relevant literature, we can assert that this is the first study of this kind so direct comparison of our results with other authors was not possible, since in most of the studies published so far, the image-based analysis has been used for identifying particle size and its distribution from loose aggregate samples (Mora *et al*., 1998; Wang, 2006; Womac *et al.,* 2007; Igathinathane *et al.*, 2009a; Igathinathane *et al.*, 2009b; Souza and Menegalli, 2011; Kumara *et al.*, 2012; Gil *et al.*, 2014; Pothule *et al.*, 2014; Pons and Dodds, 2015; Febbi *et al.*, 2015), before they are utilized in concrete mixtures, in place of directly measurements from the compact's cross sections image (Ozen and Guler, 2014).

7 Conclusions

Solid biofuels made of agricultural and forest residues as well as energy crops are with increasing interest used as environmentally friendly and renewable sources of energy possessing several benefits comparing to conventional energy sources. Currently, the production of high-quality briquettes as well as other solid bio-fuels which abound with good mechanical, chemical and energy properties is strongly desired. Presented diploma thesis was focussed on the above topics, specifically on observing and examination of briquette quality in terms of physical properties. Based on the results of analyses and measurements conducted within the research together with theoretical base and relevant findings of other authors, following conclusions were formulated. Lastly, limitations of the study as well as recommendations for future research are presented.

Briquettes made of three different sources of biomass were produced and important input parameters of feedstock materials affecting densification process, moisture content and particle size distribution, were determined. The obtained results on moisture content of all three raw materials before densification showed that they belongs to the scientists' recommended and normatively set boundary of 15%. Results from particle size distribution analysis of hemp and miscanthus showed that in their cases the method did not yield absolutely reliable results on real particle size distribution. In case of hemp it was due to the fibrous nature of this plant and in case of miscanthus it was caused by needle-like shape of particles, since this standard method did not obviate the "falling-through" effect of longer particles through smaller sieve apertures. However, these results contributed to better knowledge of input material in terms of agglomeration process.

On the bases of image-based macroscopic analysis, briquettes' surface structure was analysed and assessed. Altogether, it was detected that all scanned point of the briquette surface or better said behavioural pattern of the material at each scanned point have its different attributes which can be explicated by the demeanour of the material mass going through the pressing chamber of the piston briquetting press. The effectiveness of binding mechanisms, i.e. adhesion and bonding between surfaces of input particles, was affected, besides others, by structural and chemical composition of material, particle size and shape, particle roughness, presence of irregularly shaped particles, like fibres and elongated particles, and presence of air cavities and pores. The obtained images showed

that the bonding between particles was formed mainly through inter-particle bonds and solid bridges formed by hardening of natural binders. It was evident, that the characteristic properties of the briquette surface locations are similar for all briquettes made of different biomass sources. It was observed that the agglomeration and compaction of particles occurred unequally in different zones of the briquette outer and inner surface and zones of interaction of pressed material with piston of briquetting machine. All in all, behavioural pattern of input materials during agglomeration process in the pressing chamber of briquette machine and principles and rules in behaviour and interaction between particles at different locations on the outer surface as well as inside of the briquette were identified and contributed to the better understanding of agglomeration process during the densification in the briquetting machine.

The distribution and its sizes of particles of all three biomass sources within the meaning of lengths and areas were determined. Based on Kruskal-Wallis test we have demonstrated a statistically significant difference (with 99% confidence) in lengths and areas of particles within specified locations on the briquette surface. It was proved that the largest lengths of particles are situated at the point B, i.e. in the middle of the front side, followed by points A – top of the briquette, C – bottom of the briquette, followed by points on the rear side in the same order – E, D, and F. In case of area value, the results were analogous, the front side showed the same results, i.e. the largest particles in terms of area were located on the B, A, and C points. On the rear side, the order of points with largest particles' areas were D, E, F. Based on these findings, the set hypothesis "*the smallest particles of the biomass material are found at the bottom of the briquettes while the largest particles are present on top of the briquettes*" was partially verified. In case of briquettes made of these three biomass sources and produced under the same conditions, the smallest particles are truly situated at the bottom of the briquette, whereas the largest are located in the middle of briquette cross-section, not on the top, as was thought.

Generally, larger particle size leads to decreasing density, durability, impact resistance and increasing compressive strength (Zhang and Guo, 2014). The finer grind, the higher durability, albeit small-sized particles create more durable briquettes, fine grinding is undesirable due to increased cost of production (Kaliyan and Morey, 2009). Since we know that the particle distribution is not uniform, that the larger particles agglomerate in the middle and smaller on the bottom of briquettes, mixing of the material

during the densification could decrease this nonuniformity in distribution of larger and smaller particles, which could lead to increase the quantity of contact points for inter-bonding among particles (Drzymala, 1993; Shaw, 2008) and thus to a lower abrasion of the final products during handling.

To conclude, particle size and its distribution are major factors determining the properties of briquettes, as well as other agglomerates. Thus presented work contributes to the better understanding of raw input material agglomeration process during the briquetting which can help to improve regimes, parameters and technological aspects of briquetting equipments and, above all, can ensure high quality of biofuels with appropriate technological and mechanical properties, including density, durability, impact resistance and decreasing compressive strength, according to the given standards.

7.1 Limitations of the study

One of the limitations of this study limitation could be the small amount of examined briquettes. Although results were statistically significant, higher number of examined briquettes would be desirable. Another limitation could be chosen fraction size (i.e. 12 mm) and associated low magnification ($6.5\times$). Material with this fractional composition had to be scanned with this magnification, which not allowed capturing the particle distribution on a larger area of the cross-sectional surface. The limitation of the research may also be the fact that this is the first study of this kind, so there is not enough experience with this topic and not available precedent research methodology.

7.2 Recommendation for further research

Development of image analysis is still on the rise and it can also find application in the study of physical properties of solid biofuels. As was mentioned, image analysis has not been so far used for measuring the particle features from the image of cross sections of observed compacts. Thus, further research on the briquette surface structure based on macroscopic analysis is highly recommended, since, as was stated, they may help to better understand the interaction of input biomass particles and their behavioural pattern and agglomeration within the pressing process and thus may contribute to improvement of the production process of solid biofuels.

It is recomended to continue in studying and examining of material's particle size and its distribution and binding mechanisms between particles with utilization e.g. scanning electron microscopy with higher magnification. Further studying of lignin distribution as well as other natural binders among particles using fluorescence microscopy, which uses ultraviolet light to generate colour fluorescence according to the matter and presence of aromatic molecules in it (Rost, 1995), is recommended. It is advisable to perform a compositional analysis of an input material to detect the amount and share of the main components – cellulose, hemicelluloses, lignin and extraneous components, and thus provide complex insight to binding mechanisms. It is also recommended to determine mechanical properties including density and durability of examined briquettes, since particle size and PSD also play important roles in flow ability, compressibility of bulk solid material, and durability of densified products and since durability values represent the relative strength of the inter-particle bonding in the briquettes (Grover and Mishra, 1996; Ganesan *et al.*, 2008; Kaliyan and Morey, 2009; Kaliyan and Morey, 2010). Extension of the research on more surface zones, including lateral surfaces which are in interaction with matrix die, further on different sources of biomass and fraction size as well as different production conditions (pressure, temperature) is desirable.

References

Abdullah MZ, Aziz SA, Dos-Mohamed AM. 2000. Quality inspection of bakery products using a color-based machine vision system. Journal of Food Quality 23: 39–50.

Alaru M, Kukk L, Olt J, Menind A, Lauk R, Vollmer E, Astover A. 2011. Lignin content and briquette quality of different fibre hemp plant types and energy sunflower. Field Crops Research 124: 332–339.

Batchelor BG, Bruce G. 2012. Machine Vision for Industrial Applications. Batchelor BG, Bruce G editors. Machine Vision Handbook: Volume 1. London: Springer, p1–59.

Bato PM, Nagata M, Cao QX, Hiyoshi K, Kitahara T. 2000. Study on sorting system for strawberry using machine vision (part 2): development of sorting system with direction and judgement functions for strawberry (Akihime variety). Journal of the Japanese Society of Agricultural Machinery 62: 101–110.

BEC. Not dated. What is biomass? Available at http://www.biomassenergycentre.org.uk/portal/page?_pageid=76,15049&_dad=por tal&_schema=PORTAL: Accessed 2015-02-04.

Berrezueta E, González-Menéndez L, Ordóñez-Casado B, Olaya P. 2015. Pore network quantification of sandstones under experimental CO_2 injection using image analysis. Computers & Geosciences 77: 97–110.

BS EN ISO 16559. 2014. Solid biofuels – Terminology, definitions and descriptions. BSI. 44p.

Briklis. Not dated. Briquetting presses BrikStar CS 25, 50. Available at http://www.briklis.cz/en/briquetting-presses-for-wood/brikstar-cs-25-50/: Accessed 2015-02-13.

Brosnan T, Sun D-W. 2002. Inspection and grading of agricultural and food products by computer vision systems - a review. Computers and Electronics in Agriculture 36: 193–213.

Brožek M, Nováková A, Kolářová M. 2012. Quality evaluation of briquettes made from wood waste. Journal of Agricultural Engineering Research 58: 30–35.

Burger W, Burge MJ. 2009. Digital Image Processing: An Algorithmic Introduction Using Java. New York: Springer Science & Business Media. 586p.

Carels N. 2011. The Challenge of Bioenergies: An Overview. dos Santos Bernardes MA editor. Biofuel's Engineering Process Technology. Rijeka: InTech, p23–64.

Carlsson P, Lycksam H, Gren P, Gebart R, Wiinikka H, Iisa K. 2013. High-speed imaging of biomass particles heated with a laser. Journal of Analytical and Applied Pyrolysis 103: 278–286.

Chen L, Xing L, Han L. 2009. Renewable energy from agro-residues in China: Solid biofuels and biomass briquetting technology. Renewable and Sustainable Energy Reviews 13: 2689–2695.

Chen Y-R, Chao K, Kim MS. 2002. Machine vision technology for agricultural applications. Computers and Electronics in Agriculture 36: 173–191.

Chin OC, Siddiqui KM. 2000. Characteristics of some biomass briquettes prepared under modest die pressures. Biomass and Bioenergy 18: 223–228.

Chou C-S, Lin S-H, Peng C-C, Lu W-C. 2009. The optimum conditions for preparing solid fuel briquette of rice straw by a piston-mold process using Taguchi method. Fuel Processing Technology 90: 1041–1046.

Clifton-Brown JC, Neilson B, Lewandowski I, Jones MB. 2000. The modelled productivity of *Miscanthus × giganteus* (GREEF et DEU) in Ireland. Industrial crops and Products 12: 97–109.

Clifton-Brown JC, Stampfl PF, Jones MB. 2004 *Miscanthus* biomass production for energy in Europe and its potential contribution to decreasing fossil fuel carbon emissions. Global Change Biology 10: 509–518.

Coates W. 2000. Using cotton plant residue to produce briquettes. Biomass and Bioenergy18: 201–208.

ČSN EN 14774-2 (838220). 2010. Solid biofuels – Determination of moisture content – Oven dry method – Part 2: Total moisture – Simplified method. Czech Office for Standards, Metrology and Testing. 12p.

ČSN EN 15149-1 (838219). 2011. Solid biofuels - Determination of particle size distribution. Part 1, Oscillating screen method using sieve apertures of 1 mm and above. Czech Office for Standards, Metrology and Testing. 16p.

ČSN EN 17225-1 (838202). 2015. Solid biofuels– Fuel specifications and classes. Czech Office for Standards, Metrology and Testing. 64p.

Davies ER. 2005. Machine Vision: Theory, Algorithms, Practicalities. San Francisco: Morgan Kaufmann. 934p.

Demirbas A, Demirbas AS, Demirbas AH. 2004. Briquetting Properties of Biomass Waste Materials. Energy sources 26: 83–91.

Doehlert DC, McMullen MS, Jannick J-L, Panigrahi S, Gu H, Riveland NR. Evaluation of Oat Kernel Size Uniformity. Crop Science 44: 1178–1186.

Dowlati M, de la Guardia M, Dowlati M, Mohtasebi SS. 2012. Application of machine-vision techniques to fish-quality assessment. TrAC Trends in Analytical Chemistry 40: 168–179.

Drzymala Z. 1993. Industrial briquetting: fundamentals and methods. Michigan: Elsevies. 442p.

Du C-J, Sun D-W. 2006. Learning techniques used in computer vision for food quality evaluation: a review. Journal of Food Engineering 72: 39-55.

Dufossé K, Drewer J, Gabrielle B, Drouet J-L. 2014. Effect of 20-year old *Miscanthus × giganteus* stand and its removal on soil characteristics and greenhouse gas emissions. Biomass and Bioenergy 69: 198–210.

Erichsen JT, Woodhouse JM. 2012. Human and Animal Vision. Batchelor BG, Bruce G editors. Machine Vision Handbook: Volume 1. London: Springer, p89–115.

Faik A. 2013. "Plant Cell Wall Structure-Pretreatment" the Critical Relationship in Biomass Conversion to Fermentable Sugars. Tingyue G editor. Green Biomass Pretreatment for Biofuels Production. New York: Springer, p1–30.

Farrera-Rebollo RR, Salgado-Cruz de la Paz M, Chanona-Pérez J, Gutiérrez-López GF, Alamilla-Beltrán L, Calderón-Domínguez G. 2011. Evaluation of Image Analysis Tools for Characterization of Sweet Bread Crumb Structure. Food and Bioprocess Technology 5: 474–484.

Febbi P, Menesatti P, Costa C, Pari L, Cecchini M. 2015. Automated determination of poplar chip size distribution based on combined image and multivariate analyses. Biomass and Bioenergy 73: 1–10.

Fengel D, Wegner G. 1983. Wood – chemistry, ultrastructure, reactions. Remagen: Kessel Werlag. 613p.

Fernlund JMR. 1998. The effect of particle form on sieve analysis: a test by image analysis. Engineering Geology 50: 111–124.

Fiřt J, Holota R. 2002. Digitalizace a zpracování obrazu. Digitální mikroskopie a analýza obrazu v metalografii 1: 34–38.

Fisher RB, Breckon TP, Dawson-Howe K, Fitzgibbon A, Robertson C, Trucco E, Williams CKI. 2014. Dictionary of Computer Vision and Image Processing. London: John Wiley and Sons. 382p.

Frei M. 2013. Lignin: Characterization of a Multifaceted Crop Component. The Scientific World Journal 2013. Available at http://dx.doi.org/10.1155/2013/436517: Accessed on 2015-01-25.

Fujita M, Harada H. 2000. Ultrastructure and Formation of Wood Cell Wall. Hon DN-S, Shiraishi N editors. Wood and Cellulosic Chemistry. New York: CRC Press, p1–51.

Ganesan V, Rosentrater KA, Muthukumarappan K. 2008. Flowability and handling characteristics of bulk solids and powders – a review with implication for DDGS. Biosystems Engineering 101: 425–435.

Gevers T, Gijsenij A, Weijer J van de, Geusebroek J-M. 2012. Color in Computer Vision: Fundamentals and Applications. New Jersey: John Wiley & Sons. 284p.

Ghebre-Sellassie I. 1989. Pharmaceutical pelletization technology. New York: Marcel Dekker. 274p.

Gil M, Teruel E, Arauzo I. 2014. Analysis of standard sieving method for milled biomass through image processing. Effects of particle shape and size for poplar and corn stover. Fuel 116: 328–340.

Granada E, López González LM, Míguez JL, Moran J. 2002. Fuel lignocellulosic briquettes, die design and products study. Renewable Energy 27: 561–673.

Grover PD, Mishra SK. 1996. Biomass briquetting: technology and practise. Bangkok: FAO. 48p.

Guo Q, Chen X, Liu H. 2012. Experimental research on shape and size distribution of biomass particle. Fuel 94: 551–555.

Gutiérrez A, Rodríguez IM, Río del JC. 2006. Chemical Characterization of Lignin and Lipid Fractions in Industrial Hemp Bast Fibers Used for Manufacturing High-Quality Paper Pulps. Journal of Agricultural and Food Chemistry 54: 2138–2144.

Hiloidhari M, Das D, Baruah DC. 2014. Bioenergy potential from crop residue biomass in India. Renewable and Sustainable Energy Reviews 32: 504–512.

Hodkinson TR, Renvoize S. 2001. Nomenclature of *miscanthus × giganteus* (*Poaceae*). Kew Bulletin 56: 759–760.

Hodkinson TR, Chase MW, Renvoize SA. 2002. Characterization of a Genetic Resource Collection for *Miscanthus* (*Saccharinae, Andropogoneae, Poaceae*) using AFLP and ISSR PCR. Annals of Botany 89: 627–636.

Hong H, Yang X, You Z, Cheng F. 2014. Visual quality detection of aquatic products using machine vision. Aquacultural Engineering 63: 62–71.

Husain Z, Zainac Z, Abdullah Z. 2002. Briquetting of palm fibre and shell form the processing of palm nuts to palm oil. Biomass and Bioenergy 22: 505–509.

Igathinathane C, Melin S, Sokhansanj S, Bi X, Lim CJ, Pordesimo LO, Columbus EP. 2009a. Machine vision based particle size and size distribution determination of airbone dust particles of wood and bark pellets. Powder Technology 196: 202–212.

Igathinathane C, Pordesimo LO, Columbus EP, Batchelor WD, Sokhansanj S. 2009b. Sieveless particle size distribution analysis of articulate materials through computer vision. Computers and Electronics in Agriculture 66: 147–158.

Igathinathane C, Davis JD, Purswell JL, Columbus EP. 2010. Application of 3D scanned imaging methodology for volume, surface area, and envelope density evaluation of densified biomass. Bioresource Technology 101: 4220–4227.

Ivanova T. 2012. Research of Energy Plants Processing to Solid Biofuels [PhD]. Prague: Czech University of Life Sciences, 122p.

Jeffries TW. 1994. Biodegradation of lignin and hemicelluloses. Ratledge C editor. Biochemistry of microbial degradation. Dordrecht: Springer, p233–277.

Kaliyan N. 2008. Densification of biomass [PhD]. Minneapolis: University of Minnesota, 409p.

Kaliyan N, Morey RV. 2009. Factors affecting strength and durability of densified biomass products. Biomass and Bioenergy 33: 337–358.

Kaliyan N, Morey RV. 2010. Natural binders and solid bridge type binding mechanisms in briquettes and pellets made from corn stover and switchgrass. Bioresource Technology 101: 1082–1090.

Karakuş D, Onur AH, Deliormanli, Konak G. 2010. Size and shape analysis of mineral particles using image processing. The Journal of Ore Dressing 12: 1–8.

Karunanithy C, Wang Y, Muthukumarappan K, Pugalendhi S. 2012. Physiochemical Characterization of Briquettes Made from Different Feedstock. Biotechnology Research International 2012: 1–12.

Kers J, Kulu P, Aruniit A, Laurmaa V, Križan P, Šoos L, Kask Ü. 2010. Determination of physical, chemical and burning characteristics of polymeric waste material briquettes. Estonian Journal of Engineering 16: 307–316.

Knox JP. 2008. Revealing the structural and functional diversity of plant cell walls. Current opinion in Plant Biology 11: 308–313.

Korbářová A. 2009. Obrazová analýza opticky rozlišitelných objektů a heterogenních směsí [PhD]. Prague: Institute of Chemical Technology Prague, 189p.

Kreuger E, Sipos B, Zacchi G, Svensson S-E , Björnsson L. 2011. Bioconversion of industrial hemp to ethanol and methane: The benefits of steam pretreatment and co-production. Bioresource Technology 102: 3457–3465.

Kumar M, Turner S. 2014. Plant cellulose synthesis: CESA proteins crossing kingdoms. Phytochemistry 2014. Available at doi:10.1016/j.phytochem.2014.07.009: Accessed on 2014-11-04.

Kumara GHAJJ, Hayano K, Ogiwara K. 2012. Image Analysis Technique on Evaluation of Particle Size Distribution of Gravel. International Journal of GEOMATE 3: 290–297.

Kutay ME, Guler M, Aydilek AH. 2006. Analysis of factors affecting strain distribution in geosynthetics. Journal of Geotechnical and Geoenvironmental Engineering 132: 1–11.

Lewandowski I, Clifton-Brown JC, Scurlock JMO, Huisman W. 2000. Miscanthus: European experience with a novel energy crop. Biomass and Bioenergy 19: 209–227.

Li Y, Liu H. 2000. High-pressure densification of wood residues to form and upgraded fuel. Biomass and Bioenergy 19: 177–186.

Lindley JA, Vossoughi M. 1989. Physical properties of biomass briquettes. Transactions of the ASAE, 32, p361–366.

Lloyd BJ, Cnossen AG, Siebenmorgen TJ, 2000. Evaluation of two methods for separating head rice from brokens for head rice yield determination. Applied Engineering in Agriculture 17: 643–648.

Lu H, Ip E, Scott J, Foster P, Vickers M, Baxter LL. 2010. Effects of particle shape and size on devotilization of biomass particle. Fuel 89: 1156–1168.

Lu J, Tan J, Shatadal P, Gerrard DE. 2000. Evaluation of pork color by using computer vision. Meat Science 56: 57–60.

Mani S, Sokhansanj S, Bi X, Turhollow A. 2006a. Economics of Producing Fuel Pellet from Biomass. American Society of Agricultural and Biological Engineers 22: 421–426.

Mani S, Tabil LG, Sokhansa S. 2006b. Specific energy requirement for compacting corn stover. Bioresource Technology 97: 1420–1426.

Matiacevicha S, Silva P, Enrione J, Osorio F. 2011. Quality assessment of blueberries by computer vision. Procedia Food Science 1: 421–425.

McKendry P. 2002. Energy production from biomass (part 1): overview of biomass. Bioresource Technology 88: 37–46.

Miao Z, Phillips JW, Grift TE, Mathanker SK. 2013. Energy and pressure requirement for compression of *Miscanthus giganteus* to an extreme density. Biosystems Engineering 114: 21–25.

Mohr J, Pakr JH, Obermayer K. 2014. A computer vision system for rapid search inspired by surface-based attention mechanisms from human perception. Neural Networks 60: 182–193.

Mora CF, Kwan AKH, Chan HC. 1998. Particle size distribution analysis of coarse aggregate using digital image processing. Cement and Concrete Research 28: 921–932.

Muazu RI, Stegemann JA. 2015. Effects of operating variables on durability of fuel briquettes from rice husks and corn cobs. Fuel Processing Technology 133: 137–145.

Muntean A, Ivanova T, Havrland B, Pobedinsky V. 2012. Comparative analysis of methods for fuel biobriquettes production. Engineering for Rural Development: 496–499.

Muntean A, Ivanova T, Havrland B, Pobedinsky V, Vrancean V. 2013. Particularities of Bio-Raw Material Particle Agglomeration during Solid Fuel Pressing Process. Engineering for Rural Development: 499–503.

Ozen M, Guler G. 2014. Assessment of optimum threshold and particle shape parameter for the image analysis of aggregate size distribution of concrete sections. Optics and Lasers in Engineering 53: 122–132.

Pan S, Kudo M. 2011. Segmentation of pores in wood microscopic images based on mathematical morphology with a variable structuring element. Computers and Electronics in Agriculture 75: 250–260.

Park B, Chen YR. 2001. Co-occurrence matrix texture features of multi spectral images on poultry carcasses. Journal of Agricultural Engineering Research 78: 127–139.

Pérez J, Muñoz-Dorado J, de la Rubia T, Martínez J. 2002. Biodegradation and biological treatments of cellulose, hemicellulose and lignin: an overview. Guerrero R editor. International Microbiology. New York: Springer, p53–63.

Pietsch W. 2002. Agglomeration Processes: Phenomena, Technologies, Equipment. Weinheim: Wiley-VCH. 1104p.

Pietsch W. 2003. An interdisciplinary approach to size enlargement by agglomeration. Powder Technology 130: 8–13.

Pons M-N, Dodds J. 2015. Chapter Fifteen – Particle Shape Characterization by Image Analysis. Progress in Filtration and Separation: 609–636.

Pothula AK, Igathinathane C, Kronberg S, Hendrickson J. 2014. Digital image processing based identification of nodes and internodes of chopped biomass stems. Computers and Electronics in Agriculture 105: 54–65.

Rabier F, Temmerman M, Böhm T, Hartmann H, Jensen PD, Rathbauer J, Carrasco J, Fernández M. 2006. Particle density determination of pellets and briquettes. Biomass and Bioenergy 30: 954–963.

Rehman SUR, Rashid N, Saif A, Mahmood T, Han J-I. 2013. Potential of bioenergy production from industrial hemp (*Cannabis Sativa*): Pakistan perspective. Renewable and Sustainable Energy Reviews 18: 154–164.

Rost FWD. 1995. Fluorescence Microscopy, vol. II. New York: Cambridge University Press. 473p.

Rowell RM, Pettersen R, Tshabalala MA. 2012. Cell Wall Chemistry. Rowel RM editor. Handbook of Wood Chemistry and Wood Composites. Boca Raton: CRC Press, p34–70.

Rumpf H, 1962. The strength of granules and agglomeration. Knepper WA editor. Agglomeration. New York: John Wiley, p379–418.

Russ JC. 2006. The Image Processing Handbook, Fifth Edition. Canada: CRC Press. 832p.

Sarrafzadeh MH, La H-J, Lee J-Y, Cho D-H, Shin S-Y, Kim W-J, Oh H-M. 2015. Microalgae biomass quantification by digital image processing and RGB color analysis. Journal of Applied Phycology 27: 205–209.

Scheller HV, Ulvskov P. 2010. Hemicelluloses. Annual review of plant biology 61: 263–289.

Shah SG, Kishen JMC. 2011. Fracture properties of concrete-concrete interfaces using digital image correlation. Experimental Mechanics 51: 303–313.

Shahin MA, Symons SJ, Poysa VW. 2006. Determining Soya Been Seed Size Uniformity with Image Analysis. Biosystems Engineering 94: 191–198.

Shaw MD, Tabil LG. 2007. Compression and relaxation characteristics of selected biomass grinds. ASAE Annual International Meeting. June 17–20, 2007, Minneapolis: ASAE. Paper No. 076183.

Shaw M. 2008. Feedstock and process variables influencing biomass densification [MSc]. Saskatoon: University of Saskatchewan, p. 159.

Shen H, Li S, Gu D, Chang H. 2012. Bearing defects inspection based on machine vision. Measurement 45: 719-733.

Snyder WE, Qi H. 2004. Machine Vision. Cambridge: Cambridge University Press. 434p.

Somerville C, Youngs H, Taylor C, Davis SC, Long SP. 2010. Feedstocks for Lignocellulosic Biofuels. Science 13: 790–792.

Sonka M, Hlaváč V, Boyle R. 2014. Image Processing, Analysis, and Machine Vision. Stamford: Cengage Learning. 920p.

Souza DOC, Menegalli FC. 2011. Image analysis: Statistical study of particle size distribution and shape characterization. Powder Technology 214: 57–63.

Srivastava NSL, Narnaware SL, Makwana JP, Singh SN, Vahora S. 2014. Investigating the energy use of vegetable market waste by briquetting. Renewable Energy 68: 270–275.

Stelte W, Holm JK, Sanadi AR, Barsberg S, Ahrenfeldt J, Henriksen UB. 2011. A study of bonding and failure mechanisms in fuel pellets from different biomass resources. Biomass and Bioenergy 35: 910–918.

Stolarski MJ, Szczukowski S, Tworkowski J, Krzyzaniak M, Gulczynsk P, Mleczek M. 2013. Renewable Energy 57: 20–26.

Stupavský V, Holý T. 2010. Brikety z biomasy - dřevěné, rostlinné, směsné brikety. Biom.cz. Available at: http://biom.cz/cz/odborne-clanky/brikety-z-biomasy-drevene-rostlinne-smesne-brikety: Accessed 2015-04-02.

Suchy M. 2011. Accessibility and enzymatic degradation of native and model cellulose substrates [PhD]. Espoo: Aalto University, 162p.

Sun DW. 2000. Inspecting pizza topping percentage and distribution by a computer vision method. Journal of Food Engineering 44: 245–249.

Szeliski R. 2011. Computer Vision: Algorithms and Applications. London: Springer. 812p.

Tabil LG. 1996. Binding and pelleting characteristics of alfalfa [PhD]. Saskatoon: University of Saskatchewan, 219p.

Tabil L, Adapa P, Kashaninejad M. 2011. Biomass Feedstock Pre-Processing – Part 2: Densification. dos Santos Bernardes MA editor. Biofuel's Engineering Process Technology. Rijeka: InTech, p439–464.

Taylor S. 2007. Business Statistics for non-mathematicians. Second edition. London: Palgrave MacMillan. 368p.

Thomas M, van der Poel AFB. 1996. Physical quality of pelleted animal feed. 1. Criteria for pellet quality. Animal Feed Science and Technology 61: 89–112.

Tonar Z, Němeček S, Holota R, Kočová J, Třeška V, Moláček J, Kohoutek T, Hadravská Š. Microscopic image analysis of elastin network in samples of normal, atherosclerotic and aneurysmatic abdominal aorta and its biomechanical implications. Journal of Applied Biomedicine 1: 149–159.

Trinderup CH, Dahl A, Jensen K, Carstensen JM, Conradsen K. 2015. Comparison of a multispectral vision system and a colorimeter for the assessment of meat color. Meat Science: 1–7.

Tumuluru JS, Wright CT, Kenny KL, Hess JR. 2010. A Review on Biomass Densification Technology for Energy Application. Idaho: Idaho National Laboratory. 96p.

Tumuluru JS, Sokhansanj S, Wright CT, Boardman RD, Yancey NA. 2011a. A Review on Biomass Classification and Composition, Co-Firing Issues and Pretreatment Methods. ASABE International Meeting, Paper No. 1110458, Idaho: Idaho National Laboratory. 32p.

Tumuluru JS, Wright CT, Hess JR, Kenny KL. 2011b. A review of biomass densification system to develop uniform feedstock commodities for bioenergy application. Biofuels, Bioproducts and Biorefining 5: 683–707.

Vaezi M, Pandey V, Kumar A, Bhattacharyya S. 2013. Lignocellulosic biomass particle shape and size distribution analysis using digital image processing for pipeline hydro-transportation. Biosystems Engineering 144: 97–112.

Vanloot P, Bertrand D, Pinatel C, Artaud J, Dupuy N. 2014. Artificial vision and chemometrics analyses of olive stones for varietal identification of five French cultivars. Computers and Electronics in Agriculture 102: 98–105.

Ververis C, Georghiou K, Christodoulakis N, Santas P, Santas R. 2004. Fiber dimensions, lignin and cellulose content of various plant materials and their suitability for paper production. Industrial Crops and Products 19: 245–254.

Walker CK, Panozzo JF. 2012. Measuring volume and density of a barley grain using ellipsoid approximation from a 2-D digital image. Journal of Cereal Science 55: 61–68.

Wamukonya L, Jenkins B. 1995. Durability and relaxation of sawdust and wheat-straw briquettes as possible fuel for Kenya. Biomass and Bioenergy 8: 175–179.

Wang HH, Sun DW. 2001. Evaluation of the functional properties of cheddar cheese using a computer vision method. Journal of Food Engineering 49: 47–51.

Wang W. 2006. Image analysis of particles by modified Ferret method – best-fit rectangle. Powder Technology 165: 1–10.

Wiemann MC. 2010. Wood handbook- wood as engineering material. Madison: U. S. Department of Agriculture, Forest Service, Forest Product Laboratory. 508p.

Womac AR, Igathinathane C, Bitra P, Miu P, Yang T, Sokhansanj S, Narayan S. 2007. Biomass pre-processing size reduction with instrumented mills. ASABE Paper No. 076046, ASABE, St. Joseph, MI.

Wooten JR, Filip To SD, Igathinathane C, Pordesimo LO. 2011. Discrimination of bark from wood chips through texture analysis by image processing. Computers and Electronics in Agriculture 79: 13–19.

Wooten JR, White JG, Thomasson JA, Thompson PG, 2000. Yield and quality monitor for sweetpotato with machine vision. In: 2000 ASAE Annual International Meeting, Paper No. 001123, St. Joseph: ASAE.

Xiao-bo Z, Jie-wen Z, Yanxiao L, Holmes M. 2010. In-line detection of apple defects using three color cameras system. Computers and Electronics in Agriculture 70: 129–134.

Yaman S, Şahan M, Haykiri-açma H, Şeşen K, Küçükbayrak S. 2000. Production of fuel briquettes from olive refuse and paper mill waste. Fuel Processing Technology 68: 23–31.

Yang Z, Peng X-F, Lee D-J, Chen M-Y. 2009. An image-based method for obtaining pore-size distribution of porous media. Environmental Science & Technology 43: 3248–3253.

Zeng Y, Zhao S, Yang S, Ding A-Y. 2014. Lignin plays a negative role in the biochemical process for producing lignocellulosic biofuels. Current Opinion in Biotechnology 27: 38–45.

Zhang H, Li D. 2014. Applications of computer vision techniques to cotton foreign matter inspection: A review. Computers and Electronics in Agriculture 109: 59–70.

Zhang J, Guo Y. 2014. Physical properties of solid fuel briquettes made from *Caragana korshinskii* Kom. Powder Technology 256: 293–299.

Annexes

List of annexes

Table I: <u>Hemp</u> – All measurements of particles' areas and lengths (in µm/µm^2)

		A Area	A Length	B Area	B Length	C Area	C Length	D Area	D Length	E Area	E Length	F Area	F Length
1	1	3189877.93	3942.24	9818159.99	6125.14	4101185.36	3674.79	1329185.70	2246.49	880979.72	1848.01	2594696.63	2493.67
	2	577870.36	1486.55	1849733.82	1916.29	1695634.35	2996.86	542778.78	1714.39	2463858.05	1929.69	5711774.64	3400.59
	3	296802.27	748.17	1585841.86	3461.37	219540.41	627.25	465919.51	1653.65	4626149.97	4895.67	10224262.79	4455.61
	4	294588.08	577.09	2804440.92	3392.38	980316.39	1828.16	628293.53	1206.94	9740831.04	6454.58	5468381.34	3788.85
	5	607158.07	1490.54	7411233.49	8172.73	1849621.28	2605.53	2408637.47	2769.08	1906888.32	2335.53	2350565.27	2330.36
	6	5485477.95	4293.17	168536.35	568.54	3889461.71	3120.05	1914000.57	1398.18	1176372.96	1180.99	4256782.62	2626.30
	7	1699995.63	2670.82	1603376.38	2078.68	4815731.71	3010.93	1688991.77	3113.68	5049261.78	3604.47	930128.05	1240.86
	8	5530076.76	4397.85	1042246.65	2040.88	187770.13	585.25	4692139.58	6792.97	5930677.63	4129.07	186562.38	894.82
	9	792110.13	1971.85	210717.20	1291.51	323137.72	573.11	591524.54	1190.59	3328868.76	1746.92	636949.01	1377.13
	10	343762.34	1128.48	1821172.28	2476.73	359437.04	1122.30	11898359.10	4377.74	1917221.21	3195.68	3683575.48	4147.27
2	11	2701314.71	2628.49	1863912.88	3471.43	1602403.48	2151.63	1912021.21	3083.53	8099545.03	4497.01	1468277.16	1816.57
	12	604306.46	1483.81	9450302.32	6038.90	571731.01	835.20	2533437.33	3738.44	4420800.51	2664.22	2592918.56	1985.73
	13	512585.27	1271.72	1190563.91	2316.45	1068816.94	2043.00	710654.74	1147.37	4167544.00	4309.69	2145484.19	2579.81
	14	1182478.76	642.99	4063208.63	3349.62	2049502.36	3804.46	3320817.15	4689.54	5404169.80	4622.46	564350.37	1344.65
	15	289388.08	685.24	1521250.01	1640.17	9214021.27	6177.21	14779458.00	8214.44	6365195.88	3046.38	3097619.97	2636.30
	16	231953.30	938.85	266483.07	1388.71	2994727.17	3450.54	1457877.18	2591.30	6351742.99	2714.06	1067173.07	2047.10
	17	10057192.00	4408.71	320935.30	994.82	4034658.98	3923.72	1880318.02	1701.16	1258465.77	2235.93	14385466.16	6389.05
	18	572502.62	980.14	1047972.30	3095.27	710822.48	1452.67	1047715.03	1802.89	978873.81	754.78	508123.34	1249.32
	19	949820.94	2687.14	554352.97	1351.23	888561.65	1067.25	1026613.11	1463.76	2517501.87	2167.38	3313839.09	3018.60
	20	1788127.15	2631.18	1360262.57	2628.24	1572377.70	1265.36	1492398.43	1446.46	764768.23	1337.39	1754545.25	2125.77
	21	178980.46	825.13	1856775.83	3068.23	1223095.32	1504.42	22978462.51	9478.70	4924126.43	3086.16	7028379.70	4012.51
	22	4191329.78	2090.35	4852438.84	4856.42	1043320.19	1672.21	8805905.57	4097.03	2193659.63	1350.31	975820.91	1281.86
	23	1160530.53	1699.07	1450957.71	1309.49	612056.13	1577.38	2714866.82	2442.96	3356244.21	3197.22	1408494.00	1685.92

3	24	1345423.10	1369.36	10158709.31	3870.18	648556.74	1288.26	3664486.47	3743.25	13389985.91	8399.10	522750.42	1437.50
	25	2659713.33	1616.28	4418955.35	3308.63	927242.90	2220.43	1974085.67	3460.72	1370852.75	1732.07	559989.09	1075.18
	26	2278163.97	4287.49	13978033.18	4018.02	6398308.11	3347.40	440691.15	787.88	1037315.04	1236.34	631379.98	1261.33
	27	1340223.11	2586.76	6083568.65	3776.38	367555.74	762.03	12692985.36	6992.89	458270.49	1550.55	1265879.96	1961.30
	28	6173433.51	3566.80	2717171.27	1846.96	543181.36	1320.24	1761020.08	2540.14	107690.21	574.94	1588816.39	1822.99
	29	1653497.62	1663.32	4323727.34	4005.50	306900.32	638.83	2761700.32	3796.74	985113.80	2348.07	190823.03	593.40
	30	6052491.70	2927.06	6662061.54	3480.78	130301.80	572.28	2549238.61	3564.20	1162718.78	880.80	3208228.88	2599.30
	31	1002726.69	1472.79	1029904.83	1288.07	2776662.89	2101.45	3844708.21	4300.43	3026698.75	2897.48	7682270.63	5785.97
	32	2680077.18	3624.64	353566.08	992.48	759568.23	1545.08	1204117.44	1557.95	4746152.43	5197.59	396675.71	1516.03
4	33	1843814.19	2463.29	224841.05	1356.13	5837279.02	3903.23	1552919.66	4081.14	3561526.58	3344.69	1248334.17	1359.78
	34	2594830.82	2916.41	1142131.03	1650.86	204108.17	628.26	346554.47	1002.05	3180618.59	4080.10	736520.52	1351.79
	35	2264748.59	2154.97	1255921.63	1978.94	3481715.05	3703.96	4067033.14	4097.51	1179526.50	1425.50	2198389.95	1663.58
	36	6701484.56	8250.89	3446533.03	3479.36	1022587.31	1199.46	9137598.13	4263.19	774061.12	1810.67	6278272.10	5448.26
	37	5285583.18	3839.28	531137.83	1153.42	840453.31	1597.73	3570383.34	3826.28	3850746.92	2337.81	789292.07	2258.75
	38	509079.65	829.40	10755209.64	6745.72	603132.27	1059.48	3020056.18	4201.80	2496634.79	1587.59	2196813.17	1908.76
	39	6695915.54	3312.42	769857.26	1816.11	347997.05	828.29	4228669.10	3689.59	6017702.06	3689.76	373728.64	1442.51
	40	846391.37	1193.69	6951409.97	5346.45	300190.65	1180.90	999438.95	1280.29	3006838.13	4122.09	1726934.96	1198.75
	41	4682007.98	4041.75	4256015.51	4020.99	6170682.54	4538.89	853483.36	1240.70	1124272.37	1835.15	6736777.43	5839.45
	42	1872501.26	2552.34	2282411.04	2108.09	2860466.67	4200.41	1148997.50	1414.47	9464325.53	5854.86	2057050.74	2903.23
5	43	8151544.97	5524.56	81835.78	675.67	7293478.78	3869.86	1019098.28	1368.48	9159368.59	5303.38	798283.03	2527.35
	44	8959691.22	4489.41	8135355.26	5177.75	4098065.37	2741.57	1503066.81	1908.96	1016447.96	1858.69	469341.44	1060.10
	45	654494.80	1558.31	1125366.40	2281.47	2102507.99	2058.25	184750.77	1211.96	5558056.09	3393.93	1567177.71	2150.21
	46	1469753.29	2709.85	702763.97	865.66	3449441.53	3055.81	224908.15	891.77	1102264.65	1699.79	6371704.26	4261.29
	47	614605.81	1527.19	2491114.48	2875.26	1346496.65	2636.92	1984955.33	2154.13	710923.12	959.04	652213.51	1031.12
	48	1920240.56	2191.32	969412.01	1749.14	9868919.22	3475.13	482458.85	1535.45	2245927.96	2827.27	882053.27	979.69
	49	1698016.28	2790.59	5380349.10	3533.94	2389447.81	2751.96	1134135.58	1500.66	1001787.33	950.47	1376623.07	1077.33
	50	1354447.61	4013.57	2577702.19	2492.33	1060731.79	1156.85	1407890.13	2132.41	573106.49	1047.62	239401.04	542.90

Table II: <u>Miscanthus</u> – All measurements of particles' areas and lengths (in µm/µm^2)

		A		B		C		D		E		F	
		Area	*Length*	*Area*	*Length*	*Area*	*Length*	*Area*	*Length*	*Area*	*Length*	*Area*	*Length*
1	**1**	6663208.41	6945.08	3621826.49	4551.73	3878427.52	3641.27	1527551.31	5456.73	1167249.65	3556.23	1063742.09	2622.45
	2	1486319.04	2863.89	6025008.16	4706.02	1114298.79	2707.87	2776474.75	7614.17	10869055.56	8973.12	556353.86	1480.51
	3	577975.51	1527.16	6659982.28	5413.03	502144.84	1244.36	1236910.48	2466.43	1582139.82	3721.15	820362.62	2850.33
	4	10541870.89	5956.21	1608104.42	3689.67	1681958.12	4254.94	2694835.09	4058.18	573378.39	1449.33	199252.45	998.26
	5	5634836.46	3706.41	2050785.02	2834.88	4274337.61	4780.70	284437.67	852.65	849911.56	1633.58	1476936.67	4677.25
	6	6343276.46	5162.31	3071320.68	4469.48	1077567.71	2782.14	1124769.42	3742.89	16314070.86	6276.91	530277.49	1954.53
	7	522909.67	1285.34	2260273.98	2300.47	6076093.67	4824.57	1989096.82	2636.84	1138619.91	2010.94	138465.53	742.31
	8	476122.59	1823.19	1074385.39	1538.40	536175.55	2535.51	580706.73	2091.56	7304394.46	5005.72	438372.77	1392.58
	9	468491.04	1748.23	1571921.67	2152.81	2477552.67	4088.40	1497019.65	2591.57	3708529.39	5371.77	664541.82	1278.35
	10	1673386.46	4247.42	3231989.66	3597.29	516076.26	1306.32	162553.10	1008.93	1492554.43	1513.29	1550715.19	2322.69
2	**11**	9853326.36	7241.17	6788892.82	7454.68	6742181.06	6011.61	3708699.70	3401.15	2816783.33	3163.01	351562.53	1442.33
	12	7377091.24	5184.80	9538175.01	6566.76	1672545.73	4114.20	1711324.98	3821.44	4306945.61	3204.94	609147.58	1584.91
	13	1045820.58	2281.41	4369150.88	3266.31	4955564.02	3020.93	792838.76	1365.35	6764556.69	6051.73	331234.48	830.10
	14	1547154.47	3093.37	748094.62	1407.70	2109997.72	3829.51	1366874.03	1778.29	1563064.45	1971.83	4578553.98	4144.76
	15	809775.87	2802.78	3674025.93	5088.47	946225.36	2671.78	1802813.24	3587.06	2343021.36	4025.67	372179.74	1257.18
	16	695442.13	1990.88	14136505.87	7390.62	3659928.28	3702.57	5077211.70	3767.37	1367520.94	2454.60	849122.69	3105.55
	17	1386177.64	1931.96	1408460.19	2478.33	2718908.86	6303.36	562509.90	1026.19	655361.01	1245.03	1001048.13	2540.20
	18	2919899.75	1491.71	2109195.54	875.45	1605419.74	1957.71	637499.30	2279.01	4024059.54	5549.31	2770398.32	3067.42
	19	1036248.70	1485.86	893870.89	2251.08	1077323.15	2040.80	15206566.67	7646.47	510636.06	1249.64	174827.03	458.62
3	**20**	9875777.97	7052.46	2309916.08	4581.05	1596202.16	4424.07	2096836.48	2516.85	1389662.90	2350.90	340516.56	976.61
	21	1837793.67	2917.30	9982560.57	7930.97	3801872.54	6710.03	1052790.90	2927.21	3414120.17	6039.21	2042954.78	5581.69
	22	1152972.60	1799.43	1889609.50	2591.88	9213450.47	7508.21	391467.58	1301.34	1958731.55	2551.20	2663524.23	2552.37
	23	3325925.33	8056.29	5201438.47	5254.21	1726990.53	2863.99	7680345.80	5726.62	8964807.65	6613.58	1014956.80	3080.99
	24	2449463.59	2377.78	3748566.38	4607.62	2041112.60	3969.95	675827.77	2462.20	1602097.30	4566.62	480875.54	2591.60

	25	968092.92	2062.20	726404.77	3435.94	2699918.66	2064.17	716537.72	2380.14	1450312.60	1879.81	176070.43	1030.41
	26	1913171.98	2107.25	828277.84	3134.35	699050.96	1003.35	696487.46	1333.60	1615954.25	916.61	127375.63	1493.63
	27	957063.24	1865.41	8925858.08	6527.13	3592629.30	4787.88	210832.42	1134.68	2880787.87	2083.87	2305282.08	5735.51
	28	4600781.18	7308.79	493913.95	1665.70	1072481.30	2960.24	289174.69	1852.18	3526142.70	2806.13	188041.71	1004.24
	29	1583421.71	1924.34	2467255.18	4618.64	2593072.97	2879.65	180208.55	1316.19	445056.20	1640.12	97765.50	761.39
	30	2331053.63	3320.22	5131531.71	7110.44	1695611.61	2238.21	293196.93	1057.53	5336006.80	4614.12	437125.41	928.17
4	31	8052213.35	3334.32	25617758.23	8689.46	372008.16	1362.75	4484018.99	4147.12	3478403.31	4474.81	471165.50	1782.23
	32	12239165.21	8722.56	3207864.47	4039.99	1827390.98	2777.23	5102803.22	5381.83	5305534.10	4776.04	328316.57	1282.11
	33	1387250.30	3120.22	3887219.05	3732.79	4623224.45	8473.13	289597.42	1115.69	711556.47	1933.74	216776.99	834.71
	34	5253488.33	3770.10	2914293.91	6446.25	920954.64	912.99	671721.07	1573.60	4407199.95	4310.66	3581582.96	5311.47
	35	9524611.42	6631.35	2581198.85	3438.96	4056303.38	8906.87	1704336.70	1608.22	5111251.17	4134.33	562474.85	3028.69
	36	12216893.85	6265.76	773933.29	1792.69	1232258.97	2266.81	1710587.65	1964.71	193782.59	813.53	297582.75	1008.31
	37	538576.19	1674.87	921263.20	2107.33	2390196.99	6471.44	8193251.63	5165.97	4534406.56	4546.36	6493324.14	6759.78
	38	3209847.32	2436.51	1830606.80	3006.65	708916.87	1450.69	16603988.21	7944.90	1324750.03	1677.24	109985.62	552.14
	39	2004894.52	2834.27	303591.73	1339.64	7416148.22	5887.74	357210.42	1162.74	3145847.19	4129.46	159079.15	899.08
	40	295512.85	906.57	1888119.62	2477.48	7686111.53	6150.32	626454.49	3180.99	424914.82	1161.18	1432546.85	3594.10
5	41	6756316.57	3827.00	4992597.95	6668.93	500441.79	1144.37	4267606.05	4883.69	595445.85	941.88	3480144.10	5099.38
	42	4815274.99	4372.24	5001405.38	3864.40	4259374.41	6030.85	1322380.71	3442.34	207380.33	776.59	318964.05	1387.47
	43	5287509.64	4499.33	842712.14	2320.07	1996388.31	6159.62	460538.60	1003.42	489930.88	1543.51	373007.22	948.30
	44	7632459.73	3438.56	6521262.46	5755.16	1067052.23	1461.22	7538490.31	7468.56	516596.59	1068.76	553985.65	1656.15
	45	10906916.03	7686.40	2278945.34	4998.60	1898938.29	3126.42	2091275.28	2385.50	22051647.68	7754.45	4130705.29	6435.18
	46	2968390.54	2609.04	1742345.79	2981.32	528267.48	2567.74	488622.40	1506.93	4294715.77	4932.52	1936000.12	4225.07
	47	400821.40	1837.93	2698589.73	2435.72	608198.74	1224.79	4655061.25	4195.42	7769990.49	9039.67	2821525.35	3218.40
	48	373131.84	1339.17	710382.87	1838.76	754418.85	1830.59	442103.95	1183.93	2763018.20	4369.43	1178561.22	1269.18
	49	338638.01	1540.86	1889955.79	1903.01	4044010.76	2142.47	1481174.80	4615.16	2923676.68	5192.71	984374.16	1684.56
	50	470502.08	1645.65	2513851.59	6474.52	708623.65	1263.54	1278661.71	1888.71	10972453.40	5878.94	459165.50	1310.43

Table III: <u>Pine sawdust</u> – All measurements of particles' areas and lengths (in µm/µm^2)

		A		B		C		D		E		F	
		Area	*Length*	*Area*	*Length*	*Area*	*Length*	*Area*	*Length*	*Area*	*Length*	*Area*	*Length*
1	**1**	649669.10	1278.94	7088246.10	2490.43	898865.69	1340.20	683773.60	1240.39	2452533.18	2120.46	2200016.26	4037.79
	2	1761928.17	1055.50	3875974.31	3218.61	8860024.41	6125.91	488328.76	1783.34	611679.57	1507.50	4289938.80	3002.88
	3	1163182.14	1557.81	2616253.81	1713.42	14428040.54	5782.60	296680.62	821.76	1316509.15	1350.99	925399.33	1985.01
	4	6719655.09	4449.46	4543082.17	3609.86	4166203.56	2451.17	674196.86	490.46	550469.87	806.19	1954689.53	2101.41
	5	466971.72	1607.64	1260789.94	1852.71	5114551.99	1955.66	463735.24	826.64	956039.72	1065.49	1062572.44	1161.67
	6	2552144.04	1548.26	8647945.62	3436.89	585758.82	2319.68	42330.33	273.72	6972841.00	3761.34	883345.66	1024.48
	7	4811008.69	2922.07	4376727.35	2603.37	600861.99	744.80	1152523.87	1774.87	500639.62	1362.88	576755.55	1294.96
	8	1739827.45	1138.07	1553395.43	1169.49	1805566.85	4143.24	115034.22	798.65	544543.66	657.50	3408642.54	3938.91
	9	730330.98	1035.35	566101.69	570.33	2506104.08	2177.99	57205.44	307.03	3551845.16	1342.49	7687951.79	3746.68
	10	2665323.91	2638.61	3442174.09	1747.43	1361934.21	1485.99	160594.57	547.37	82577.44	480.72	121980.23	534.84
	11	796172.71	1177.66	7464855.95	4294.21	7992487.96	5607.53	1805475.95	2879.56	1063572.19	2671.70	576090.18	1398.08
2	**12**	1269701.89	2660.69	11898591.33	4702.85	2657855.57	907.29	6989417.18	6018.01	749685.67	1293.55	279579.48	528.86
	13	9230920.36	4492.56	3263792.51	2134.57	6360157.73	3176.61	9976859.23	6339.67	375007.88	1273.53	755502.20	1734.70
	14	2590180.41	2853.69	4336880.56	1699.06	1601734.79	1249.88	1103890.56	1918.81	770591.27	778.85	499819.32	911.08
	15	7408775.71	3762.19	5487638.94	2167.38	548151.87	1232.39	3443434.68	1586.46	1300163.02	875.69	451918.96	818.52
	16	8965266.70	4569.37	2352261.00	2127.91	563689.28	1877.04	2996478.84	2082.52	755159.64	662.90	478226.65	765.27
	17	3596118.81	2120.88	2681279.18	1917.54	611655.03	1585.74	98534.59	340.54	1254060.68	1738.21	77744.31	371.86
	18	446393.22	1239.39	3447387.19	4210.79	680205.74	1054.61	71115.54	367.84	110799.66	578.03	1825035.70	2031.13
	19	2165667.24	1251.02	2747026.30	2668.03	1987547.53	1135.20	5293015.64	3330.32	2218853.94	3441.36	218819.97	646.71
	20	1791844.78	3785.72	2425806.24	2879.04	2521064.34	1788.80	2103765.03	3217.91	173901.55	587.05	160605.50	832.96
3	**21**	3626083.34	3335.08	3429918.06	1386.94	4902771.39	2723.09	462421.92	946.72	510023.56	962.11	2547685.69	2427.09
	22	4064626.79	1451.89	5223205.20	1783.56	1404598.63	1397.59	603250.80	1071.61	1641619.37	2695.49	276448.20	656.56
	23	1314065.86	2187.52	8494540.38	3311.61	3612066.75	2344.37	130922.45	940.18	477088.56	809.43	138648.82	461.71
	24	2957899.79	3089.69	1040606.34	1783.15	582328.53	811.20	290916.89	634.98	725700.91	874.43	806738.82	945.28

25	1556989.98	1812.28	2358711.49	2480.89	10719007.03	4509.09	233448.35	746.09	778744.46	840.05	3154479.76	2711.51
26	1221618.16	1349.55	3465986.68	2273.80	442435.46	1974.66	59128.99	323.95	232862.03	601.36	401423.94	1390.16
27	4549963.00	1895.56	15137851.51	5818.95	2464526.22	1524.35	281657.75	814.27	746057.72	1136.25	83161.89	401.50
28	2273900.58	1762.92	297303.95	601.02	2178902.98	1976.12	105424.66	416.67	324881.42	1107.25	241786.00	1220.22
29	1034617.79	1111.99	1855337.61	1205.13	2071269.06	1378.31	125744.09	538.99	276582.27	611.20	326400.14	1243.13
4 30	1479738.97	1504.97	3052826.83	2700.67	728340.69	1653.43	120903.45	861.06	298704.44	381.47	94012.67	427.16
31	1400667.20	1814.52	1959973.42	1528.52	3360449.55	3166.17	180168.29	608.60	3958368.89	2158.39	855278.47	1393.66
32	2417259.24	3634.02	2460287.27	1868.00	1436491.38	1626.42	281846.33	579.91	531962.08	1187.65	464971.41	1358.49
33	2775903.13	2089.90	17075639.76	4176.10	1614943.84	1113.43	611837.02	1128.53	173502.83	790.07	2966104.97	2931.16
34	1074814.75	1303.96	3412407.93	2201.91	5325065.25	5331.95	173811.68	649.55	271324.22	733.71	3275160.44	2834.99
35	4041223.28	2453.93	2495874.21	2798.54	358628.40	1340.75	770890.33	1191.87	1444906.99	2638.77	90588.04	529.10
36	2658569.90	1472.47	2530186.14	2135.06	2021236.79	855.25	63317.31	515.31	205041.32	493.06	1098543.28	1647.52
37	6424946.47	2246.23	862558.31	1514.38	511058.89	681.75	66081.05	534.32	8947260.17	4843.78	654749.00	1016.73
38	5576263.81	3553.91	3067673.61	2007.87	1304997.13	1224.61	137385.57	489.22	128674.87	491.39	820790.78	1264.38
39	336305.61	734.33	2597393.32	1046.83	309438.13	1348.23	140923.16	402.09	1700064.65	2210.72	344468.64	680.58
40	519021.26	820.98	3205629.67	2707.94	425731.72	1301.54	769314.99	1125.59	167666.42	303.92	198406.31	876.87
41	5088687.97	3457.68	3647169.60	2126.28	4122883.73	2455.72	920788.79	1613.93	7298046.78	2739.45	639206.40	966.88
5 42	5331196.38	2485.30	5581090.06	2607.79	869756.48	940.44	533803.84	1553.74	1207943.15	1318.06	542114.40	1486.21
43	4650132.99	2414.77	1119144.91	1407.81	1282555.25	1131.09	1278144.11	1415.82	555960.99	701.25	128694.83	749.07
44	4036314.19	3768.21	1426891.47	2601.60	976741.83	1301.54	82852.16	601.94	212317.75	394.57	129129.15	735.09
45	14343949.35	3991.58	901710.08	1221.38	1528785.10	1284.37	517050.65	894.09	1294318.49	2112.89	911016.05	2266.53
46	3873514.47	2402.80	3359855.05	2196.38	1603229.31	2094.63	317839.94	877.56	769481.04	2063.46	144927.58	534.60
47	746527.98	910.11	4702147.88	5857.68	1495059.62	1839.90	255922.35	786.48	247758.69	1202.45	337820.53	879.36
48	1459970.48	1096.29	1204447.13	2650.50	753860.39	1185.55	547372.55	719.00	7183608.34	2964.36	376828.01	1296.16
49	3808078.14	3002.67	265334.66	602.69	598373.51	1107.21	89553.44	329.51	379193.48	916.60	248703.23	528.86
50	2391534.10	1252.70	3767960.48	2263.27	731386.13	816.05	169165.73	863.59	860938.89	1088.48	112977.82	557.70

Notices: colors separate individual measurements made on one briquette; that applies also to previous Tables I and II.
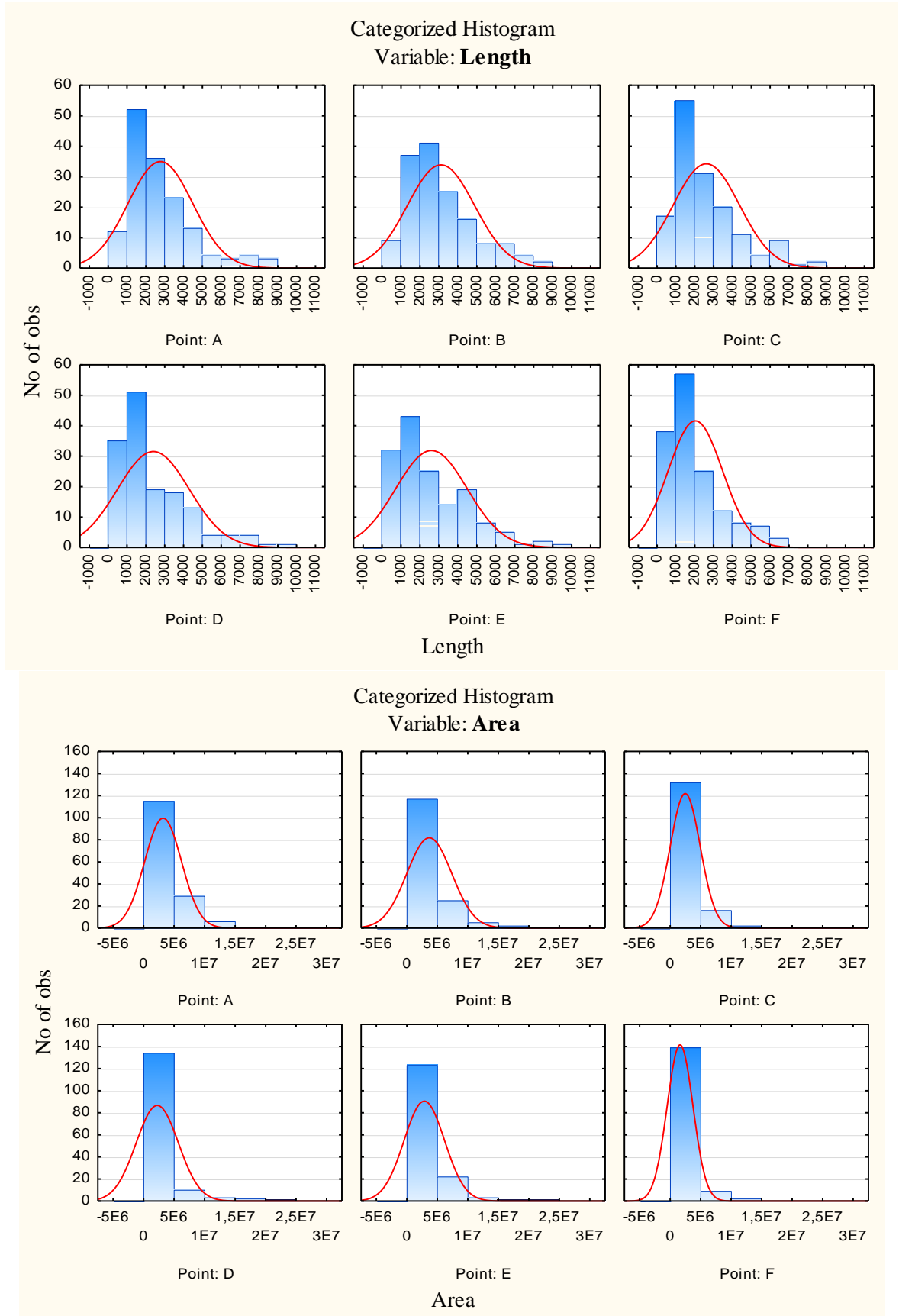
Figure I: Histograms for length and area variable according to points

Notices: the comas in area histogram labels are meant as point, i.e. decimal mark; E notation in area histogram labels means 10^x – e.g. in case of $1.5E7 = 1.5 \times 10^7$